# The Simulation of Electrolyte Systems: The System K-Na-Mg-Cl-$SO_4$-$H_2O$

Venasan Pillay

Department of Chemical Engineering
University of Cape Town
Rondebosch, 7700
South Africa

31 August 2004

A thesis submitted for the degree of Master of Science at the University of Cape Town

# Acknowledgements

I wish to thank and acknowledge the people who have contributed to the completion of this thesis:

To my supervisor, A/Prof. A.E. Lewis for her supervision, advice and most importantly for the opportunities presented to me over the period of my postgraduate studies in her group.

To Marcelo Seckler, Gert-Jan Witkamp, Chrismono Himawan and most of all to Robert Gärtner (my German taskmaster) for the insight and direction during my time at TU Delft.

To 'La Famiglia', those individuals who became my family in Delft, Mahery, Pascal, Laura S., Laura C., Stefania, Alex, Maria, Sylvain, Jordi and Lydia. Thanks for the adventures and great experiences together.

To the members of the precipitation group for providing a stimulating and enjoyable environment to work in. Special mention must go to Rob van Hille for his input and Fran Pocock for always being on hand to provide help when needed. Thanks to Jeeten and Eugene who have been a great source of council, advice and laughter.

Thanks to my friends who have been supportive and understanding whenever I have been too busy and ended up neglecting them. There are too many to mention but you know who you are!

To CALTEX, my bursar company who have provided financial support and allowed me the opportunity to further my studies.

Finally, eternal gratitude to my parents and brothers, Kuben and Desh, who have supported and helped me get through my studies and the journey of my life thus far. Thanks for always being there.

# Synopsis

Aqueous electrolyte solutions are encountered in many industrial processes such as wastewater treatment, seawater desalination, distillation and biological processes (Myers and Sandler, 2002; Sandler, 1999). A detailed knowledge of the thermodynamic properties of these electrolyte solutions is essential for process development, design and improvement.

However, these solutions have intrinsic complexities that result in deviations from ideality. This non-ideality is described mathematically by the activity coefficient ($\gamma$), which deviates from the ideal case value of unity with increasing non-ideality. This non-ideality increases with increasing molality (Sandler, 1994) and is generally described by derivations from the excess Gibbs free energy ($G^{ex}$) (Renon, 1986).

There are a number of approaches available to describe this behaviour, ranging from empirical methods to integral equation theory (Gui-Wu et al., 2004). Empirical or semi-empirical models can be effectively used to carry out engineering investigations.

The objectives of this work were to carry out a critical review of relevant literature on existing models and to thereafter select and input this model into mathematical modelling software in order to set up a simulator. Once the simulator converged to a solution, it was shown that the simulator predictions are accurate. Thereafter, the simulator was applied to two industrial issues so that its usefulness could be demonstrated.

The salient findings of the literature review are summarised as follows:

- The Debye-Hückel theory was an early development that introduced the important concept of the theoretical limiting law (Renon, 1986) that has since been used in the development of subsequent models;

- The graphical model proposed by Meissner and Tester (1972) uses the concept of the family of curves, which can be used to determine the mean ionic activity coefficient of a number of salts. For the purposes of simulation such a model is ineffectual. Further to this the model is predictive and extrapolative and is of limited accuracy and is of better use when used in collaboration with other methods (Sandler, 1994);

- The model proposed by Bromley (1973) is a generalised analytical correlation that allows the determination of a number of thermodynamic properties. The Bromley model is merely a representation of the Meissner and Tester curves. The major limitation of the Bromley model is that extension to multi-component systems is largely empirical and inconsistent (Renon, 1986).

- The Pitzer model is the most popular approach for predicting thermodynamic properties of aqueous electrolyte solutions (Renon, 1986; Chen et al., 1982; Jin and Donahue, 1988). It is semi-empirical and based on the ion-interaction approach. It comprises of a set of theoretically and empirically derived equations (Pitzer and Pabalan, 1987). Expressions for activity and osmotic coefficients are derivatives of the virial $G^{ex}$ (Spencer et al., 1990). These expressions are given in terms of six empirical parameters that are widely available in literature.

- Other models of interest include local composition models, mean spherical approximation (MSA) models, the Helgeson-Kirkham-Flowers (HKF) model. Renon (1985) carried out a direct comparison of these models against that of the Pitzer model and revealed that the predictions of the Pitzer model were most accurate.

Based on these findings, the relatively simplistic form, applicability, accuracy and general availability of parameters, the Pitzer model was selected for the simulator. The Pitzer approach requires the simultaneous solution of a system of non-linear equations. An investigation into viable mathematical modelling software alternatives, lead to the selection of the software package g-PROMS. The main criteria in making the choice were a user-friendly language and reasonable computing power.

Extensive work has been done on improving the Pitzer model in terms of applicability and accuracy. Spencer, Møller and Weare (SMW) (1990) model proposed a modified Pitzer model that included temperature dependency and focused particularly on parameter estimation in the low temperature range (< 25°C). Visual and statistical analyses of the predictions of this model reveal that it is of high accuracy.

Marion and Farren (1999) recognised that the parameterisation and validation of the SMW model focused on chloride chemistry. This led them to investigate and re-evaluate the sulphate salt parameterisation of the SMW model, which serves as basis for the FREZCHEM model. The results from that work showed an improvement in predictions for sulphate salts. The parameters of the SMW model in conjunction with the improved sulphate parameters of the FREZCHEM model were used in the simulator of this work.

In order to show the applicability and use of the simulator two case study investigations were carried out. The first of the case studies was a theoretical investigation of the system $MgSO_4$-$H_2O$. Recent interest to recover magnesium sulphate heptahydrate ($MgSO_4.7H_2O$), for use as a fertilizer by crystallization from solutions of eutectic composition has risen (Himawan *et al.*, 2002; Genceli *et al.*, 2003). However, $MgSO_4.12H_2O$ crystallizes at the eutectic and has to be subsequently converted to $MgSO_4.7H_2O$ by solution-mediated recrystallization therefore detailed knowledge of the phase diagram in the system Mg-$SO_4$-$H_2O$ is needed. This can be achieved by simulation.

The solid phase, $MgSO_4.12H_2O$ is of particular interest as experimental data for it is scarce. The solubility of a solid phase can be expressed thermodynamically as its solubility product. In the Pitzer model this solubility product is expressed as an empirical correlation. In this work, new correlations for the two solid phases are proposed in order to improve accuracy in the prediction of the phase diagram.

The second case study concerns NEDMAG, a producer of high-grade synthetic dead-burned magnesia and other magnesium compounds. They make use of solution mining to obtain their products. An internal investigation of the brines exiting the mine caverns has revealed an increase in KCl and NaCl. Specifications limiting the allowable concentration of NaCl and KCl in the final product of NEDMAG require a lowering in concentration of the NaCl and KCl.

A possible solution to the NEDMAG problem would be to design a process that would induce crystallisation of solid phases containing KCl and NaCl in their structure. In order to examine the viability of a cooling crystallisation process, an examination of the resulting 3-dimensional phase diagram of the system was used. The temperature range of investigation was from 0°C to 70°C and at each stage there will exist a solubility surface.

Before the simulator could be applied to the case studies, it was necessary to verify that the predictions were accurate. Use was made of both visual and statistical methods to verify the simulator. Also the parameters used in the simulator were estimated for low temperatures while the second case study is at high temperatures therefore it was necessary to check whether the expected deviations were substantial enough to preclude applying the simulator to the second case study.

From the verification process it was found that the simulator predictions for all the solid phases of interest were accurate. A sigma value ($\sigma$) and an $R^2$ value provided a numerical indication of the quality in prediction. The $\sigma$ values, which represent the model prediction deviation from experimental data, were found to range from 0.016 to 0.104m. The

$R^2$ values, which represent the degree of correlation, ranged from 0.974-0.999. This verified that the simulator predictions were accurate. There were deviations at higher temperatures but they were found to be not significant enough to eliminate the use of the simulator in application to the second case study.

The results for the first case study revealed accurate predictions of the epsomite and $MgSO_4.12H_2O$ solubility lines when the new proposed correlations were used. Further to this an improvement in prediction in comparison to the original FREZCHEM model predictions was observed. It was experimentally determined (Himawan, 2002) that the eutectic point occurs at 17.4 wt-% and –3.7°C. The simulator predicts the eutectic as 17.3 wt-% and –3.7°C while the FREZCHEM prediction is 17.3 wt-% and –3.6°C. This means that an improved solubility diagram of the system was obtained.

In the second case study, the simulation and examination of the 3-dimensional solubility surfaces reveals that there is a potential crystallisation route to reduce the concentrations of KCl and NaCl. The crystallisation of carnallite ($KCl.MgCl_2.6H_2O$) will lead to a decrease in KCl concentration while the crystallisation of halite (NaCl) will decrease the NaCl concentration. However the close proximity of the feed concentrations to the $NaCl/KCl.MgCl_2.H_2O$ eutectic point adds greater complexity to the problem meaning that an optimum separation process can only be designed with an accurate knowledge of the thermodynamics of the system.

Suggested future work includes using the simulator and improved predicted phase diagram to design the crystallisation process required in the first case study, the inclusion of high temperature parameters to increase applicability of the simulator, design of the cooling crystallisation process required for the second case study and the estimation of Pitzer parameters over a wide temperature range.

# Contents

# List of Tables

# List of Illustrations

# Nomenclature

$a_i$ – the activity of species i [mol/kg $H_2O$]

aw – the activity of water [mol/kg $H_2O$]

a1, a2, a3, a4, a5, a6 – values of fitting constants

A, $A_\Phi$ – Debye-Hückel parameter

b – constant in the Pitzer equations [$kg^{0.5}/mol^{0.5}$]

B – empirical parameter of the Bromley model

B – parameter required for calculation of the dielectric constant

$B_{MX}^{\phi}$, $B_{ca}^{\phi}$ – ion binary interaction parameter for the osmotic coefficient used in the Pitzer model

$B_{MX}$ – ion binary interaction parameter in the Pitzer model

$B_{MX}^{'}$ – derivative of the ion binary interaction parameter in the Pitzer model

C – parameter required for calculation of the dielectric constant

$C^{\phi}$, $C_{MX}^{\phi}$ – ion binary interaction parameter in the Pitzer model

$C_{MX}$, $C_{ca}$ – ion binary interaction parameter in the Pitzer model

$d_w$ – density of water [g/l]

e – elementary charge [C]

$f'$ – ionic strength dependence of the ionic activity coefficient

g(x) – ionic strength dependence fit function

g'(x) – derivative of the ionic strength dependence fit function

$G_i^{ex}$, $G^{ex}$ – excess Gibbs free energy [J/mol]

I – ionic strength [mol/kg]

k – Boltzmann constant [J/K]

$K_{sp,i}$ – solubility product of salt i

$m_a$ – molality of anion [mol/kg $H_2O$]

$m_c$ – molality of cation [mol/kg $H_2O$]

$m_i$ – molality of species i [mol/kg $H_2O$]

$m_{i,observed}$ – the ith experimentally determined solubility [mol/kg $H_2O$]

$m_{i,predicted}$ – the ith predicted solubility [mol/kg $H_2O$]

$M_w$ – molecular weight of water [g/mol]

n – number of data points

$N_o$ – Avogadro's constant [particle/mol]

P – pressure [atm]

P(T) – temperature dependent parameter

R – universal gas constant [J/mol K]

R – Pearson product moment correlation coefficient for statistical analysis

T – temperature [°C, K]

$U_1$, $U_2$, $U_3$, $U_4$, $U_5$, $U_6$, $U_7$, $U_8$, $U_9$ – parameters required for the calculation of the dielectric constant [K]

X – first data set

Y – second data set

$z_m$, $z_+$ – charge of cation (metal)

$z_x$, $z_-$ – charge of anion

$z_i$ – charge of ionic species

Z – reduced ionic strength

## Greek symbols

$\alpha_1$, $\alpha_2$ – constant in the Pitzer equations [$kg^{0.5}/mol^{0.5}$]

$\beta_{MX}^{(0)}$, $\beta_{MX}^{(1)}$, $\beta_{MX}^{(2)}$ – solute specific temperature dependant binary interaction parameters in the Pitzer model

$\varepsilon$ – dielectric constant

$\varepsilon_o$ - vacuum permitivitty [$C^2/J\ m$]

$\varepsilon_{1000}$ – parameter required for calculation of the dielectric constant

$\gamma_i$ – activity coefficient of ionic species i

$\gamma_\pm$ – mean ionic activity coefficient of species i

$\theta_{cc'}$, $\theta_{ij}$ – solute specific temperature dependant binary interaction parameters in the Pitzer model

$\Phi_{cc'}$ – interaction parameter in the Pitzer model accounting for cation-cation interaction

$\Phi'_{cc'}$ – derivative of the interaction parameter in the Pitzer model accounting for cation-cation interaction

$\Phi^{\phi}_{cc'}$ – interaction parameter in the Pitzer model accounting for cation-cation interaction for the osmotic coefficient

$\phi$ – the osmotic coefficient

$\Gamma_{ij}$ – reduced activity coefficient

# Chapter 1

# Introduction

## 1.1 Background

### 1.1.1 Electrolyte solutions

Solutions containing ionic species (aqueous electrolyte solutions) are encountered in many industrial processes such as wastewater treatment, seawater desalination, distillation and biological processes (Myers and Sandler, 2002; Sandler, 1999). They are common in the environment as well as in living organisms (Jin and Donohue, 1988). Electrolyte solutions have intrinsic complexities such as long-range inter-ionic interactions, ionic solvation, ionic pairing and partial dissociation of electrolytes (Gui-Wu et al., 2004).

Electrolyte solutions deviate significantly from ideality due to coulombic and damped coulombic force interactions between the charged particles (Sandler, 1999). Even for dilute electrolyte solutions some non-ideality is observed. This is described mathematically by the activity coefficient ($\gamma$), which deviates from the ideal case value of unity with increasing non-ideality.

A detailed knowledge of the thermodynamic properties of these electrolyte solutions is essential since they are evident in many industrial processes such as petrochemical refining, purification processes in environmental engineering, and fermentation processes in biological engineering resulting in better process design, optimisation and control (Myers and Sandler, 2002; Jin and Donohue, 1988).

### 1.1.2 Describing the thermodynamic behaviour

According to Renon (1986), describing deviation from ideality is generally derived from the excess Gibbs free energy ($G^{ex}$). The thermodynamic properties that can be derived from this approach are the activity coefficients of molecular solutes, excess partial molar volumes, enthalpies, entropies and heat capacities.

The activity of a species ($a_i$) relates directly to the excess Gibbs free energy ($G_i^{ex}$) by the following relation:

$$G_i^{ex} = R \cdot T \cdot \ln(a_i) \qquad (1.1)$$

where R is the universal gas constant [J/mol K] and T is the temperature [K].

The activity coefficient of a dissolved species relates to its activity as:

$$a_i = \gamma_i m_i \qquad (1.2)$$

where $m_i$ is the molality of the species. Defined in this way, the activity coefficient of the species approaches unity as molality approaches zero (i.e. approaches infinite dilution) (Sandler, 1994). In other words, the activity coefficient of a species deviates from ideality (unity) at high molalities.

There are a number of approaches taken to describe the thermodynamic behaviour of electrolyte solutions including integral equation theory, perturbation theory, fluctuation theory and semi-empirical theories (Gui-Wu et al., 2004). Essentially there are two categories of models: empirical and molecular (Renon, 1986).

Empirical models are used to represent experimental data while molecular models are used for understanding the effect of various different forces on the structural and thermodynamic properties (Renon, 1986). For the purposes of an engineering investigation, the empirical models will suffice.

## 1.2 Objectives

The objectives of the work undertaken in this investigation are:

- To carry out a critical review of relevant literature on existing empirical and semi-empirical models
- To determine the most suitable model for the simulation of electrolyte solutions on the basis of accuracy, applicability and ease of input
- To set up a simulator of the selected model using appropriate mathematical modelling software
- To demonstrate the accuracy and applicability of the simulator by investigating two pertinent industrial issues

## 1.3 Plan of Development

In the following two chapters, a review of the literature will be carried out in order to demonstrate the logic and decision making process used in setting up the simulator. This will include discussion on the existing empirical models that can be used to describe the thermodynamic behaviour of electrolyte solutions.

Thereafter the selected model will be discussed in greater detail with emphasis on displaying the accuracy and applicability of that model. Any necessary equations and parameters will also be reported in this section.

An introduction to the two industrial issues will be followed by a comprehensive description on the research methods for this work. A presentation of the results along with their discussion will illustrate the success of the work. Relevant conclusions will then be drawn from these results.

# Chapter 2

## Existing Models

An examination of some of the existing models is necessary in order to determine the model best suited for this investigation.

### 2.1 Debye-Hückel theory

The Debye-Hückel theory is the most basic model describing electrolyte solutions but it established the important concept of the theoretical limiting law (Renon, 1986). The Debye-Hückel limiting law is expressed as:

$$\log \gamma_{\pm} = -A \cdot |z_{+} \cdot z_{-}| \cdot \sqrt{I} \qquad (2.1)$$

where $\gamma_{\pm}$ is the mean ionic activity coefficient, A is the Debye-Hückel parameter, $z_+$, $z_-$ are the charges of the cations and anions of the electrolyte and I is the ionic strength.

The limitation of the theory is that it only accounts for long-range interactions and is thus only applicable to dilute solutions. Many models have their basis in Debye-Hückel and are an extended form of the theory with either the addition of a polynomial of ionic strength or by the consideration of solvation equilibria for applicability to higher concentrations (Renon, 1986).

### 2.2 Meissner and Tester model

The Meissner and Tester model is graphical in nature and uses the concept of a family of curves. The mean activity coefficient of an electrolyte ($\gamma_{\pm}$) in aqueous solution is known to vary with ionic strength (I) (Meissner and Tester, 1972). Values for $\gamma_{\pm}$ can be obtained from standard references (Harned and Owen, 1958; Robinson and Stokes, 1965). The reduced activity coefficient is defined as:

$$\Gamma_{ij} = \gamma_{ij}^{1/z_+ z_-} \qquad (2.2)$$

where $\Gamma_{ij}$ is the reduced activity coefficient, $z_+$, $z_-$ are the charges of the cations and anions of the electrolyte and $\gamma_{\pm}$ is the mean ionic activity coefficient

By plotting the reduced activity coefficient against ionic strength for an electrolyte, the formation of a curve family is observed such that with a known value of ($\gamma_{\pm}$), its value at any other ionic strength can be determined.

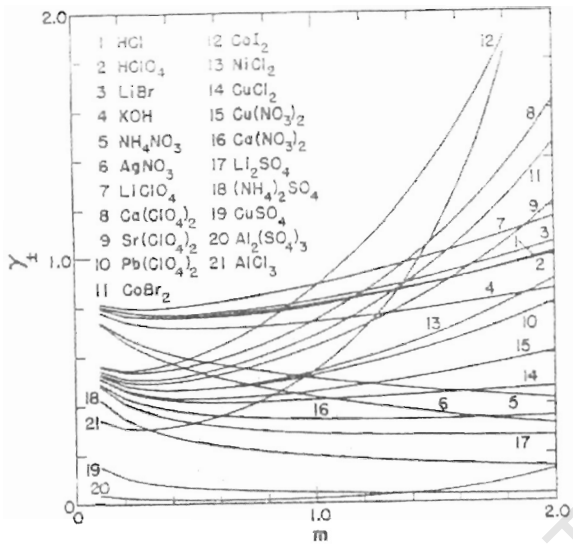


Figure 2.1: The effect of concentration on the mean activity coefficient ($\gamma_{\pm}$) for aqueous solutions at 25°C (Meissner and Tester, 1972)

Figure 2.1 shows that the change of the mean activity coefficient with molality differs significantly from electrolyte to electrolyte (Meissner and Tester, 1972). This is a useful observation and leads on to figure 2, in which log ($\Gamma$) is plotted against ionic strength. In Figure 2.2, the electrolytes as in Figure 2.1 have curves that do not cross each other. Thus for any electrolyte the mean ionic activity coefficient can be determined if another point on the curves is known.

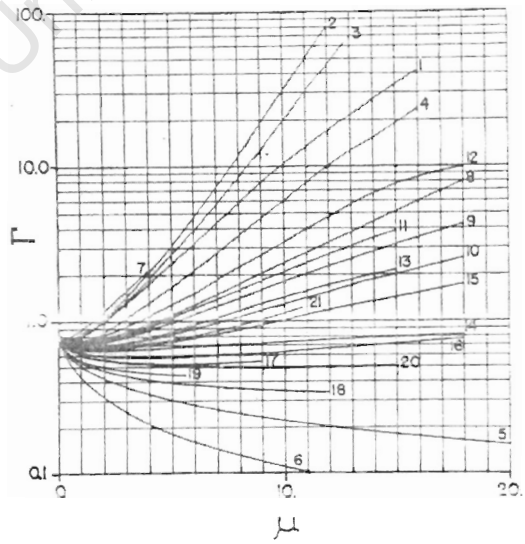


Figure 2.2: The effect of ionic strength on $\Gamma$ at 25°C (line numbers correspond to that of Figure 2.1) (Meissner and Tester, 1972)

For simulation purposes the model is limited because of its graphical nature. Some temperature considerations have been considered in order to expand the usefulness of the model (Meissner et al., 1972) but the core of it is still graphical.

The Meissner and Tester model (1972) can be used over a wide concentration range up to an ionic strength of 20 and is thus more useful than the Debye-Hückel model. The curves diverge at low ionic strengths and this makes the determination of the mean activity coefficient difficult in this region.

In summary, the model is a predictive and extrapolative approach that is of limited accuracy and is of better use when used in collaboration with other methods (Sandler, 1994).

## 2.3 Bromley model

The model proposed by Bromley (1973) is a generalised analytical correlation that allows the determination of a number of thermodynamic properties viz. the activity coefficient ($\gamma_{\pm}$), osmotic coefficient ($\phi$), enthalpies and heat capacities. The Bromley model is merely a representation of the Meissner curves in terms of a Debye-Hückel term with a one-parameter (B) term (Renon, 1986). The mean ionic activity coefficient ($\gamma_{\pm}$) is correlated by a single parameter equation:

$$\log \gamma_{\pm} = \frac{-A_{\Phi} \cdot |z_{+}z_{-}| \cdot I^{0.5}}{1 + I^{0.5}} + \frac{(0.06 + 0.6 \cdot B) \cdot |z_{+}z_{-}| \cdot I}{(1 + \frac{1.5}{|z_{+}z_{-}|} \cdot I)^{2}} + B \cdot I \qquad (2.3)$$

where B is the empirical parameter. Values for this parameter are tabulated in literature for a number of salts at 25°C (Bromley, 1973). $z_{+}$, $z_{-}$ are the charges of the cations and anions of the electrolyte and I is the ionic strength. The long-range interaction forces are accounted for by a Debye-Hückel parameter ($A_{\Phi}$). Using rigorous thermodynamics, it is possible to obtain equations for a number of other useful thermodynamic properties eg. the osmotic coefficient ($\phi$) (Bromley, 1973).

The Bromley model is applicable up to an ionic strength of 6. Some temperature dependency has been taken into account by variation of B with temperature. The major limitation of the Bromley model is that extension to multi-component systems is empirical and inconsistent (Renon, 1986).

## 2.4 Pitzer model

The Pitzer model is the most popular approach for predicting thermodynamic properties of aqueous electrolyte solutions (Renon, 1986; Chen et al., 1982; Jin and Donahue, 1988). It is semi-empirical and based on the ion-interaction approach. It is made up of a set of theoretically and empirically derived equations that account for the interactions between the particular aqueous ions and forces arising from the solvent (Pitzer and Pabalan, 1987).

The model is a virial expansion of excess Gibbs energy ($G^{ex}$) in terms of ion molalities. Expressions from theoretical considerations have also been considered during this development. The regression of numerous binary and ternary data was necessary in the development (Renon, 1986). Expressions for activity and osmotic coefficients are derivatives of the virial $G^{ex}$ (Spencer et al., 1990).

The equations for the activity coefficients of the relevant ions in solution are given in terms of six empirical parameters:

$$\beta_{MX}^{(0)}, \beta_{MX}^{(1)}, \beta_{MX}^{(2)}, C_{MX}^{\phi}, \theta_{ij}, \Psi_{ijk}$$

These parameters are widely available in literature (Spencer et al., 1990; Marion, 2002; Marion and Farren, 1999). The Pitzer approach uses a form of Debye-Hückel theory to account for long-range interactions. This is also extended further to account for binary and ternary interactions.

The major advantage of the Pitzer model is its flexibility (Renon, 1986). However, it is limited to aqueous solutions with a maximum applicable molality of 6M (Watanasiri and Liu, 1999).

## 2.5 Other Models of interest

The four models that have been discussed thus far are considered the most important and popular. There are however many more models that have been developed that deserve mention in this review.

### 2.5.1 Local Composition models

The local composition models are a family of models that have been developed by another extension of the Debye-Hückel theory (Renon, 1986). An example of this type is the model of Cruz and Renon (1978), which was further modified by Ball et al. (1985a). The approach proposed by Cruz gives the excess Gibbs energy ($G^{ex}$) as:

$$G^{ex} = G^{ex}_{Debye-Huckel} + G^{ex}_{Debye-Mcaulay} + G^{ex}_{NRTL} \qquad (2.4)$$

The first two terms account for long-range coulombic interactions between ions, while the NRTL term accounts for short-range effects. The Debye-Mcaulay term is necessary to counteract the effect of neglecting the variation of the dielectric constant with ionic concentration (Ball et al., 1985a), which is a major assumption of this model. Due to a large number of parameters, ion-ion and ion-solvent short-range interactions are ignored. Expressions for each of these terms are reported elsewhere (Ball et al., 1985a; Cruz and Renon, 1978). The relevant thermodynamic properties can be determined since the $G^{ex}$ can be determined.

The Chen-NRTL model (Chen et al., 1982; Chen et al., 1986) is another example of a local composition model but ion-ion and ion-solvent short-range interactions are not neglected. The assumptions in the Chen-NRTL model are:

1. Absence of ion-ion interaction for ions of same sign
2. Local electro neutrality around a solvent

This serves to reduce the number of parameters (Renon, 1986). The Chen-NRTL model is used in Aspen Plus (Aspen Plus, 1994). This model is not limited to water solvent systems and can be applied to mixed solvent systems. Its applicability range essentially spans the entire concentration range (Watanasiri and Liu, 1999).

### 2.5.2 Mean Spherical Approximation (MSA) models

The mean spherical approximation models make use of a more exact description of inter-particle interactions. Both short range and electrostatic effects are considered (Renon, 1986). These models require the mean spherical approximation of the solution of the integral equations of statistical mechanics. This results in the determination of the structure of the liquid and the thermodynamic properties.

The model proposed by Planche and Renon (1981) uses the MSA approach. The work of Ball et al. (1985b) re-examines the Planche model (1981) and proposes improvements and validations.

### 2.5.3 Helgeson-Kirkham-Flowers (HKF) model

The Helgeson-Kirkham-Flowers equation of state is the model used by the aqueous chemistry package OLI. Helgeson et al. (1974, 1976, 1981) have determined that for any aqueous species, its thermodynamic properties can be expressed by seven parameters that have specific values for each species (Berthold, 2000).

These parameters are the property of OLI systems Inc. and are thus not readily available.

### 2.5.4 Comparison to Pitzer

Renon (1985) carried out a review of existing electrolyte models in which the following table was presented.

Table 2.1: Average deviations (percent) on osmotic coefficients (Renon, 1985)

| Solution of | Pitzer | Chen-NRTL | Ball-Cruz-NRTL | Ball-Planche-MSA |
|---|---|---|---|---|
| 1-1 Electrolytes | 0.5 | 0.9 | 0.6 | 1.4 |
| Other salts | 1.8 | 5.5 | 2.4 | 2.0 |
| Two salts | 1.4 | 1.8 | 1.9 | 2.0 |

The average standard deviation between experimental and predicted values of the osmotic coefficient ($\phi$) from the Pitzer, Chen-NRTL, Ball-Cruz-NRTL and Ball-Planche-MSA models were compared. This is useful because the accuracy of prediction by the different approaches can be compared against each other.

The predictions for 1-1 electrolytes for all the salts were found to be below 1.5% for all of the models. In general the Pitzer predictions were the best.

# Chapter 3

## The Pitzer approach in more detail

The Pitzer approach is made up of a set of theoretically and empirically derived equations that account for the interactions between the particular aqueous ions and forces arising from the solvent (Pitzer and Pabalan, 1987).

The literature on existing models has shown that Pitzer has substantial applicability and accuracy. Its semi-empirical nature makes it relatively simplistic. The general availability of the Pitzer parameters also increases its attractiveness. A further examination of the Pitzer approach is undertaken with emphasis placed on understanding the equation parameters.

### 3.1 The Pitzer equations

The main variables to be calculated from the Pitzer approach are the activity coefficients of the ionic species. This is important for the calculation of the activities of the species as described by eqn. 1.2. This in turn is used for the calculation of the solubility products and therefore the solubilities.

The activity coefficient of the cation:

$$\ln \gamma_M = z_M^2 F + \sum_a m_a (2B_{Ma} + ZC_{Ma}) + \sum_c m_c (2\Phi_{Mc} + \sum_a m_a \Psi_{Mca})$$
$$\sum_{a<a'} \sum m_a m_{a'} \Psi_{Maa'} + z_M \sum_c \sum_a m_c m_a C_{ca}$$

(3.1)

The activity coefficient of the anion:

$$\ln \gamma_X = z_X^2 F + \sum_c m_c (2B_{cX} + ZC_{cX}) + \sum_a m_a (2\Phi_{Xa} + \sum_c m_c \Psi_{cXa})$$
$$\sum_{c<c'} \sum m_c m_{c'} \Psi_{cc'X} + |z_X| \sum_c \sum_a m_c m_a C_{ca}$$

(3.2)

$m_i$ represents molalities of the ionic species. $A_\Phi$ is a Debye-Hückel interaction term. The terms B, C, $\Phi$ and $\Psi$ are interaction parameters that account for the different interactions present in electrolyte solutions.

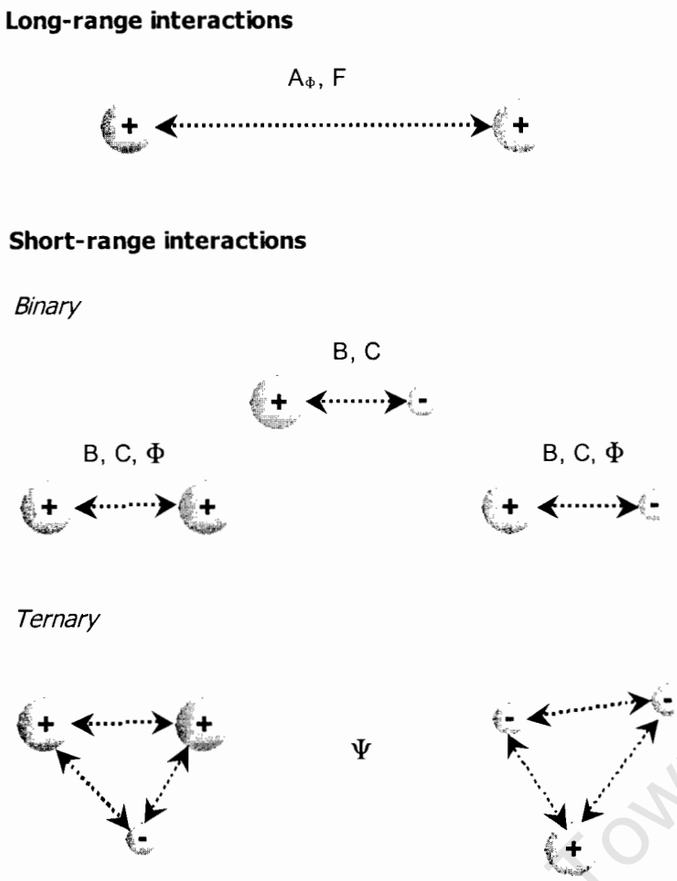


Figure 3.1: Interactions of ions in solution

Figure 3.1 gives a visual representation of the forces existing between ions in solution. Large and small circles represent the cations and anions respectively, while the arrows indicate the forces experienced between them. The Pitzer parameters corresponding to the respective forces are also shown on the diagram. The terms $A_\Phi$ and F are Debye-Hückel terms accounting for the long-range interactions between ions (cation-cation, anion-anion or cation-anion).

The parameters, B, C and $\Phi$ account for any short-range binary interactions occurring. As illustrated in the diagram this applies to cation-cation, anion-anion and cation-anion interaction. The parameter, $\Phi$ accounts specifically for cation-cation and anion-anion interaction. The effects of ternary interactions are accounted for by the parameter, $\Psi$. Cation-cation-anion and anion-anion-cation are the interactions shown in the diagram. Higher order interactions are neglected.

The osmotic coefficient:

$$(\phi - 1) = \left(2 / \sum_i m_i\right) \cdot [-A_\Phi I^{3/2} / \left(1 + bI^{1/2}\right) + \sum_c \sum_a m_c m_a \left(B^\phi_{ca} + ZC_{ca}\right)$$
$$+ \sum_{c<c'} \sum m_c m_{c'} (\Phi^\phi_{cc'} + \sum_a m_a \Psi_{cc'a}) + \sum_{a<a'} \sum m_a m_{a'} (\Phi^\phi_{aa'} + \sum_c m_c \Psi_{caa'})]$$

(3.3)

Calculation of the osmotic coefficient is important for the overall simulator because it is used to determine the activity of water ($a_w$) by eqn. 3.4.

The activity of water:

$$\ln a_w = -\phi \cdot (M_w / 1000) \cdot \sum_i m_i \qquad (3.4)$$

The activity of water is then used in the calculation of the solubility product ($K_{sp}$), which relates to the solubility. Consider the salt $M_aX_b.nH_2O$. The solubility product of this salt in terms of the activities of the species is defined as:

$$K_{sp} = a_M^a \cdot a_X^b \cdot a_w^n \qquad (3.5)$$

*Debye-Hückel parameter*

The dielectric constant is necessary for the calculation of the Debye-Hückel parameter. The equations required are given below.

Dielectric constant:

$$\varepsilon = \varepsilon_{1000} + C \ln[(B + P) / (B + 1000)] \qquad (3.6)$$

Dielectric constant parameter 1:

$$\varepsilon_{1000} = U_1 \exp(U_2 T + U_3 T^2) \qquad (3.7)$$

Dielectric constant parameter 2:

$$C = U_4 + U_5 /(U_6 + T) \tag{3.8}$$

Dielectric constant parameter 3:

$$B = U_7 + U_8 / T + U_9 T \tag{3.9}$$

Debye-Hückel parameter:

$$A_\phi = (1/3) \cdot (2\pi N_o d_w / 1000)^{1/2} (e^2 / \varepsilon\varepsilon_o kT)^{3/2} \tag{3.10}$$

*Other terms*

The equations given here are mainly for the calculation of the Pitzer parameters.

Ionic strength dependence of the ion activity coefficients:

$$F = -A_\phi I^{1/2} /(1 + bI^{1/2}) + (2/b)\ln(1 + bI^{1/2}) \tag{3.11}$$

Ion-binary interaction parameter for the osmotic coefficient:

$$B^{\phi}_{MX} = \beta^{(0)}_{MX} + \beta^{(1)}_{MX} \exp(-\alpha_1 I^{1/2}) + \beta^{(2)}_{MX} \exp(-\alpha_2 I^{1/2}) \tag{3.12}$$

Ion-binary interaction parameter:

$$B_{MX} = \beta^{(0)}_{MX} + \beta^{(1)}_{MX} g(\alpha_1 I^{1/2}) + \beta^{(2)}_{MX} g(\alpha_2 I^{1/2}) \tag{3.13}$$

Ionic strength dependence fit function:

$$g(x) = 2[1 - (1 + x)\exp(-x)] / x^2 \tag{3.14}$$

Derivative of $B_{MX}$:

$$B'_{MX} = [\beta^{(1)}_{MX} g'(\alpha_1 I^{1/2}) + \beta^{(2)}_{MX} g'(\alpha_2 I^{1/2})] / I \quad (3.15)$$

Derivative of g(x):

$$g'(x) = -2[1 - (1 + x + x^2/2)\exp(-x)] / x^2 \quad (3.16)$$

Ion-binary interaction parameter:

$$C_{MX} = C^{\phi} / 2|z_M z_X|^{1/2} \quad (3.17)$$

Ionic strength:

$$I = \frac{1}{2}\sum_i m_i z_i^2 \quad (3.18)$$

Reduced ionic strength:

$$Z = \sum_i m_i |z_i| \quad (3.19)$$

Cation-cation interaction:

$$\Phi_{cc'} = \theta^{(0)}_{cc'} + (2\theta^{(1)}_{cc'} / \alpha^2 I)[1 - (1 + \alpha I^{1/2})\exp(-\alpha I^{1/2})] \quad (3.20)$$

Derivative of cation-cation interaction:

$$\Phi'_{cc'} = -2\alpha\theta^{(1)}_{cc'} / 3 \quad (3.21)$$

Cation-cation interaction for the osmotic coefficient:

$$\Phi^{\phi}_{cc'} = \Phi_{cc'} + I\Phi'_{cc'} \quad (3.22)$$

## 3.2 Modified Pitzer models

Due to the relative simplicity and wide ranging applicability of the Pitzer framework, extensive work has been done on increasing its applicability as well as improving the quality of the predictions (Spencer et al., 1990; Marion and Farren, 1999; Marion, 2002; Marion, 2001; Marion et al.; 2003; Pitzer, 1973; Pitzer and Pabalan, 1987; Pitzer and Kim, 1974; Harvie et al., 1984; Harvie et al., 1982; Christov, 2001; Pérez-Villaseñor et al., 2002). This has led to the development of many modified Pitzer models. An examination of two such models will be carried out here. This will also serve to highlight the accuracy of prediction of the Pitzer model. The parameters of these two modified models will be used in the simulator.

### 3.2.1 The Spencer, Møller and Weare (SMW) model

Harvie, Møller and Weare (HMW model) (1984), using Pitzer as their basis, developed a geochemical model that accurately predicts mineral solubilities in complex brines. Their models apply from low to high concentrations but only at 25°C. Due to the varying physical conditions under which electrolyte solutions are encountered, an incorporation of temperature dependency into the Pitzer model is useful.

There has been work done on development of variable temperature models by generation of parameters at temperatures greater than 25°C (Pitzer and Pabalan, 1987; Møller, 1988; Greenberg and Møller, 1989)

Spencer, Møller and Weare (1990) identified the need for low temperature parameters. They state that modern evaporite systems are situated in areas that are subject to temperatures below 25°C. They give the example of hydrohalite and sylvite, which are minerals that precipitate at low temperatures.

This led to the development of the Spencer-Møller-Weare (SMW) model, which is essentially an extension of the HMW model to lower temperatures. They consider the system Na-K-Ca-Mg-Cl-$SO_4$-$H_2O$ in the temperature range – 60 to 25°C.

### 3.2.2 Verification of SMW

In order to show the accuracy of the SMW model, several curves are presented here to give a visual impression of the predictions against experimental data. Thereafter a discussion will follow regarding the statistical analysis that was carried out in the verification of the model (Spencer et al., 1990). The points and lines represent the experimental data and model predictions respectively.

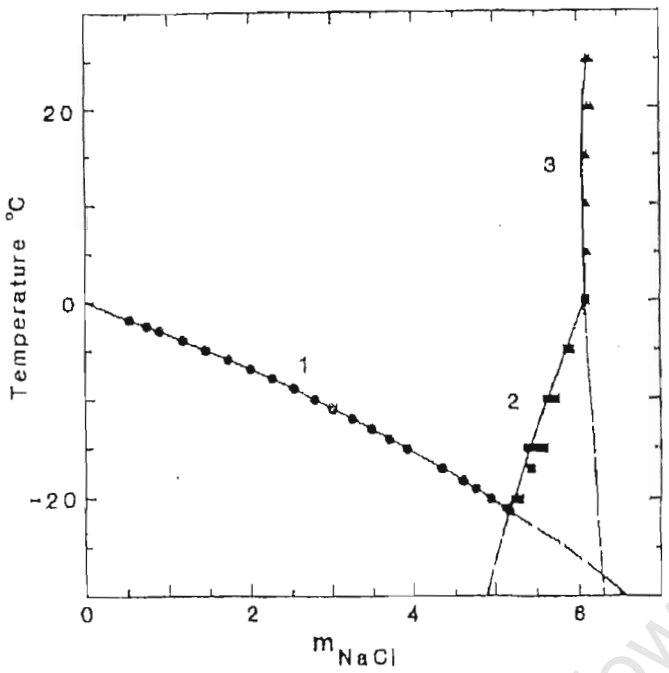


Figure 3.2: The system NaCl-$H_2O$: model prediction vs. experimental data for solid phases ice (1, circles), hydrohalite (NaCl.2$H_2O$) (2, squares) and halite (NaCl) (3, triangles) (Spencer et al., 1990)

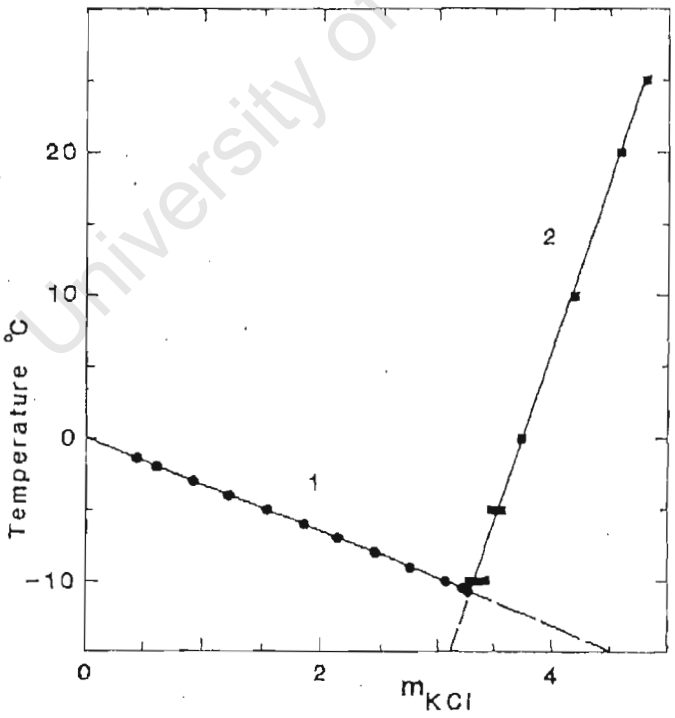


Figure 3.3: The system KCl-$H_2O$: model prediction vs. experimental data for solid phases ice (1, circles) and sylvite (KCl) (2, squares) (Spencer et al., 1990)

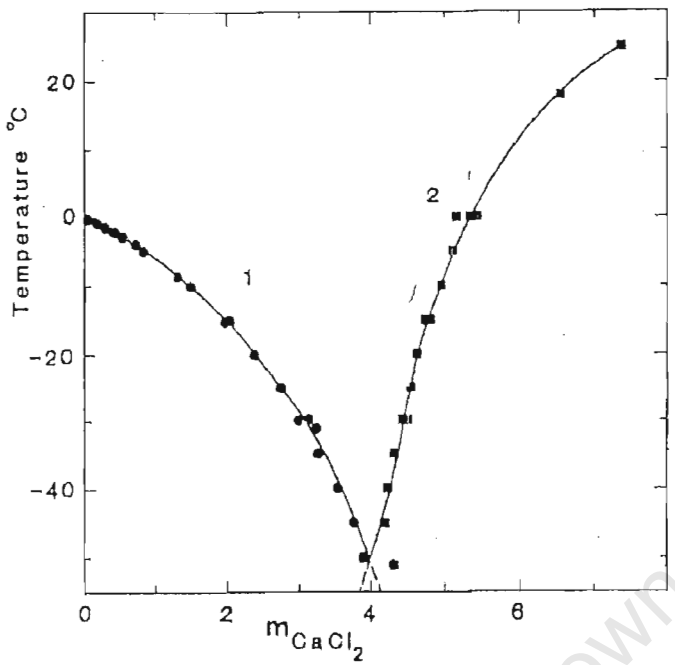


Figure 3.4: The system $CaCl_2$-$H_2O$: model prediction vs. experimental data for solid phases ice (1, circles) and antarcticite ($CaCl_2.6H_2O$) (2, squares) (Spencer et al., 1990)

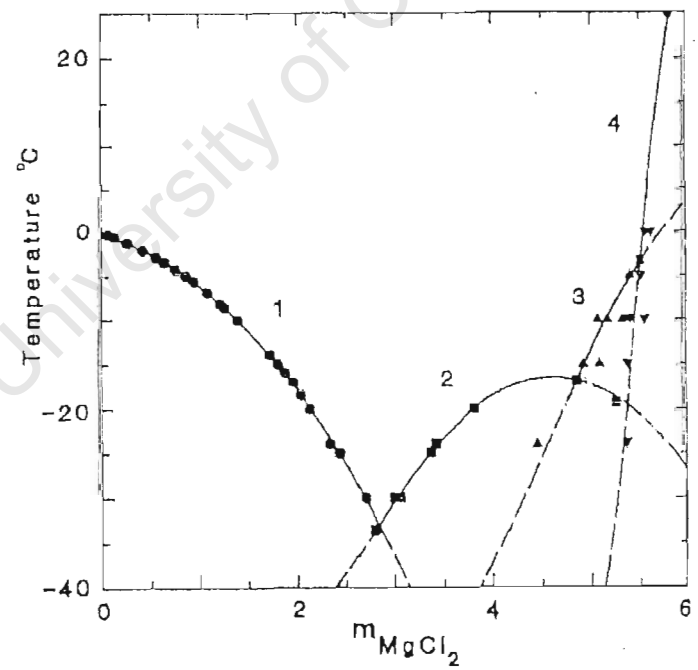


Figure 3.5: The system $MgCl_2$-$H_2O$: model prediction vs. experimental data for solid phases ice (1, circles), $MgCl_2.12H_2O$ (2, squares), $MgCl_2.8H_2O$ (3, triangles) and bischofite ($MgCl_2.6H_2O$) (4, inverted triangles) (Spencer et al., 1990)

The figures presented are the solubility diagrams of different systems under consideration. They comprise the solubility lines for the individual solid phases that are present in the

systems. From the figures presented it can be observed that the model predictions are in good agreement with the experimental data. The experimental data used in the graphs were taken from Hall et al. (1988), Yanetieva (1946), Gibbard and Fong (1975) and the compilation by Bukshtein et al. (1953).

The SMW model is also applicable to multi-component systems.

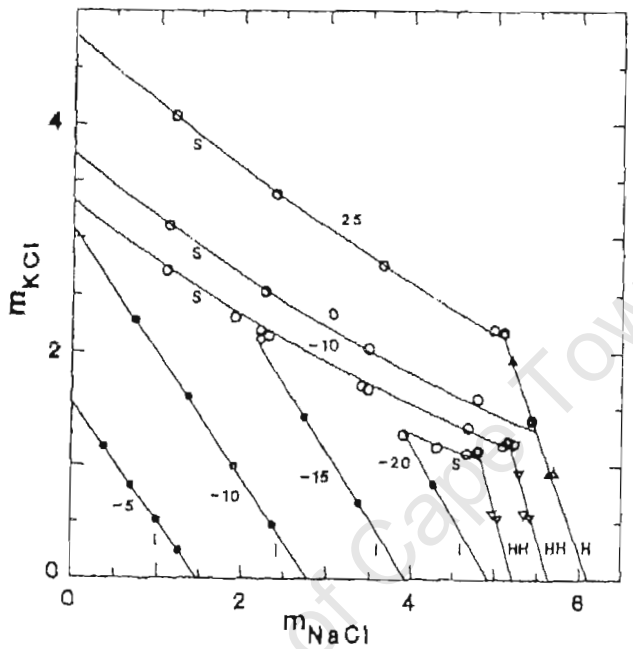


Figure 3.6: The system NaCl-KCl-$H_2O$-model prediction vs. experimental data (S – sylvite, H –halite, HH – hydrohalite) (Spencer et al., 1990)

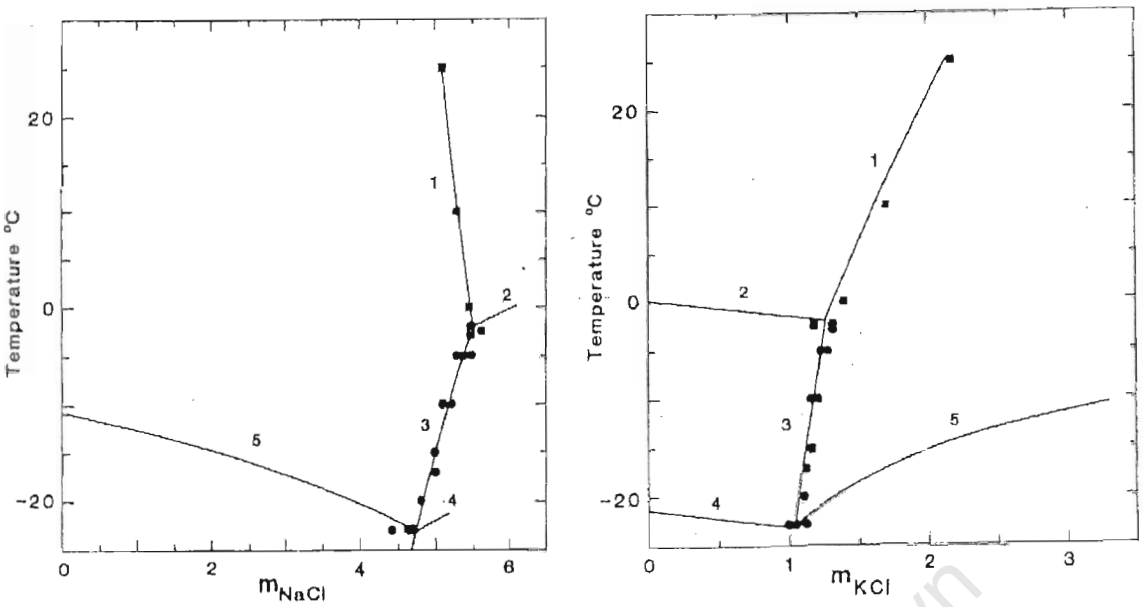


Figure 3.7: The system NaCl-KCl-$H_2O$: model prediction vs. experimental data (Spencer et al., 1990)

Figures 3.6 and 3.7 show that for multi-component systems the predictions of the model are close to the measured data. In Figure 3.7 the curves and data represent the equilibria among aqueous solutions and halite-sylvite (1), hydrohalite-halite (2), hydrohalite-sylvite (3), hydrohalite-ice (4) and sylvite-ice (5).

### 3.2.3 Statistical verification

Spencer et al. (1990) also carried out a statistical analysis to verify the model. A sigma value ($\sigma$) was used to represent the relative errors of the models predictions to the experimental data.

This value is defined as:

$$\sigma = \frac{\sqrt{\sum (m_{i,observed} - m_{i,predicted})^2}}{n} \qquad (3.23)$$

where $m_{i,observed}$ is the ith experimentally determined solubility, $m_{i,predicted}$ is the ith solubility calculated by the model and n is the number of data points.

The sigma values for the solid phases apparent in the systems are presented in Table 3.1. The sigma values are all low indicating that the model predictions are close to experimental solubility data. This sigma is useful because it provides a numerical indication of the quality of the predictions.

Table 3.1: Sigma values for the SMW model (Values taken from Spencer et al., 1990)

| System | σ |
|---|---|
| *$NaCl$-$H_2O$* | |
| Ice | 0.00039 |
| Halite | 0.022 |
| Hydrohalite | 0.026 |
| *$KCl$-$H_2O$* | |
| Ice | 0.00046 |
| Sylvite | 0.027 |
| *$CaCl_2$-$H_2O$* | |
| Ice | 0.014 |
| Antarcticite | 0.123 |
| *$MgCl_2$-$H_2O$* | |
| Ice | 0.0029 |
| Bischofite ($MgCl_2.6H_2O$) | 0.104 |
| $MgCl_2.8H_2O$ | 0.089 |
| $MgCl_2.12H_2O$ | 0.029 |

### 3.2.4 The FREZCHEM model

The accuracy of prediction of Pitzer depends on the quality of the parameters. Many studies have been done to improve the parameters and therefore to improve the accuracy.

Marion and Farren (1999) recognised that the parameterisation and validation of the SMW model focused on chloride chemistry. This led them to investigate and re-evaluate the sulphate salt parameterisation of the SMW model, which serves as basis for the FREZCHEM model.

The majority of parameters as defined in the SMW model are part of the FREZCHEM model. This is especially so for the chloride salt parameters which have been shown to generate accurate predictions. This is done to minimise changes to the original model thus allowing seamless integration of the two.

### 3.2.5 Verification of FREZCHEM

As with the SMW model, curves are presented again to give a visual representation of the model accuracy. Thereafter a brief discussion will follow. The curves presented also show the comparison between SMW model predictions and the FREZCHEM model. This is useful in showing the improvements that have been made to the SMW model.

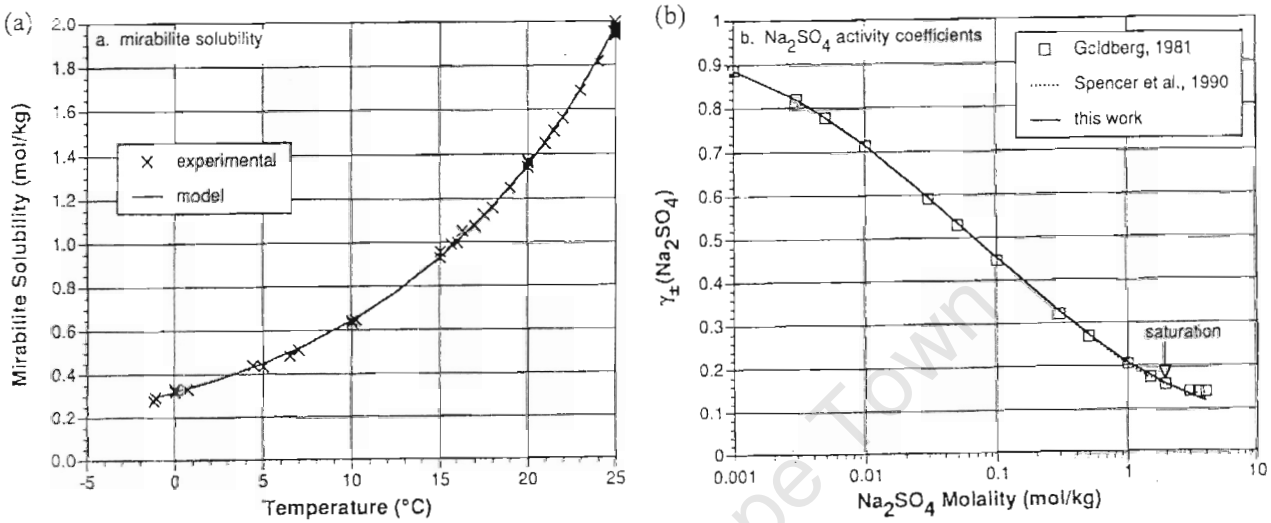


Figure 3.8: The system $Na_2SO_4$-$H_2O$: model prediction vs. experimental data for mirabilite ($Na_2SO_4.10H_2O$) (Marion and Farren, 1999)

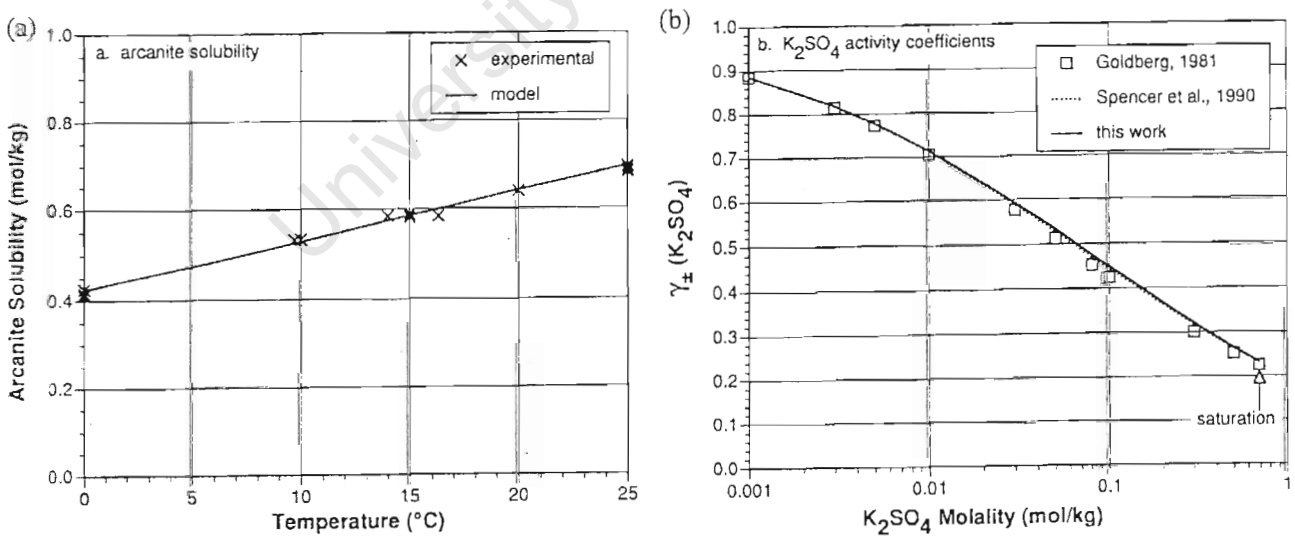


Figure 3.9: The system $K_2SO_4$-$H_2O$: model prediction vs. experimental data for arcanite ($K_2SO_4$) (Marion and Farren, 1999)

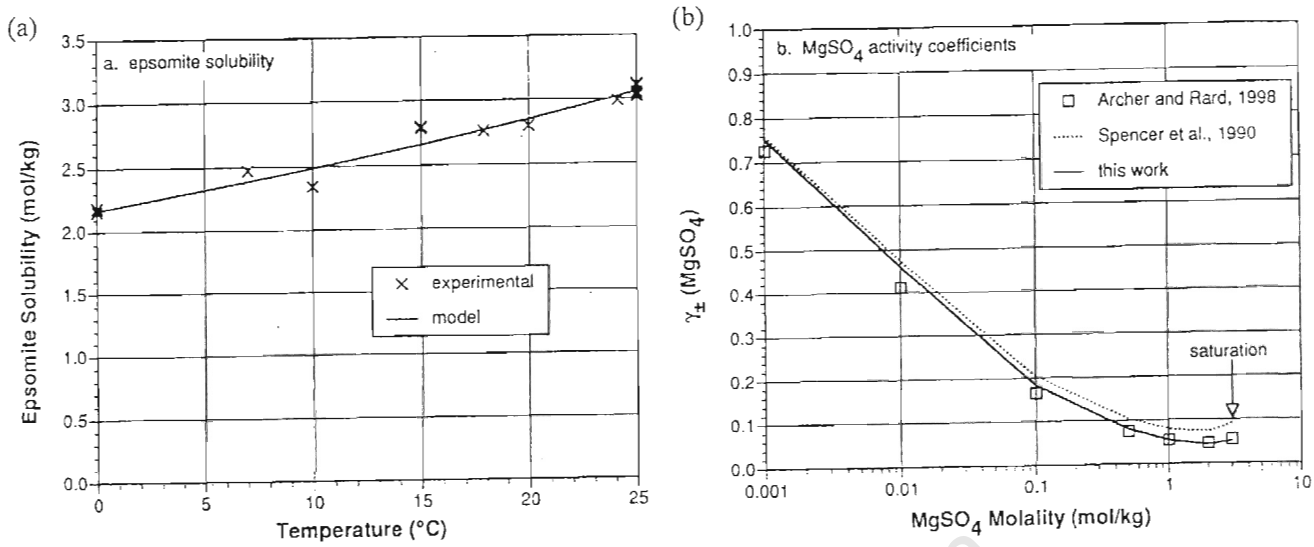


Figure 3.10: The system $MgSO_4$-$H_2O$: model prediction vs. experimental data for epsomite ($MgSO_4.7H_2O$) (Marion and Farren, 1999)

The work of Marion and Farren (1999) deals specifically with improvement of sulphate salt predictions; hence the curves that have been presented are for sulphate salts. The predicted values compare well with experimental data and show a distinct improvement from the SMW model predictions. This improvement can be noted especially in Figure 3.10b. The solubility lines of solid phases are presented in Figures 3.8a, 3.9a and 3.10a. Figures 3.8b, 3.9b and 3.10b are predictions of activity coefficient data.

The model estimates are all in good agreement with measured data. The activity coefficient estimates for the $MgSO_4$-$H_2O$ system show an improvement from the SMW predictions. FREZCHEM is also applicable to multi-component systems.

Figure 3.11 illustrates the quality of prediction of multi-component systems.

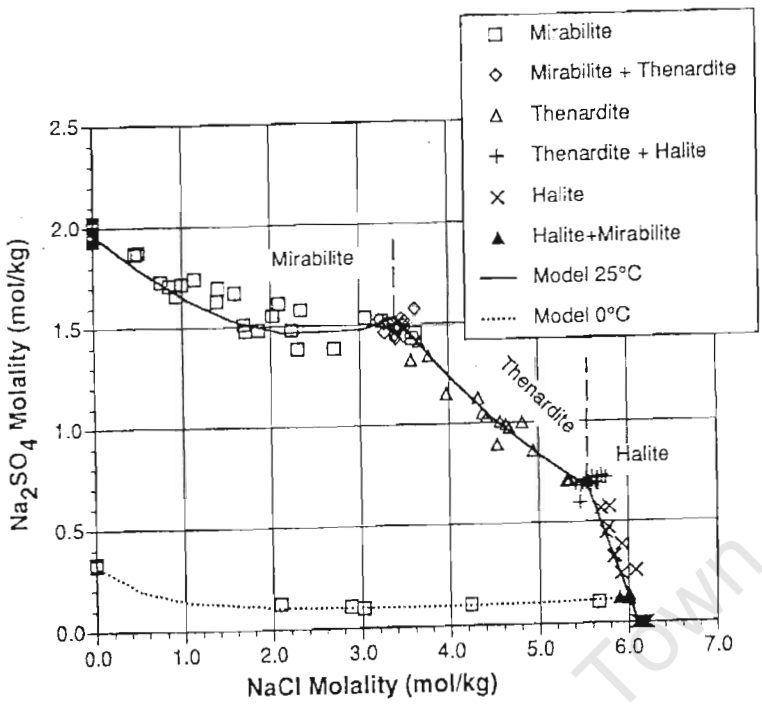


Figure 3.11: The system NaCl-Na2$SO_4$-$H_2O$: model prediction vs. experimental data (Marion and Farren, 1999)

# Chapter 4

## The Case Studies

In order to show the applicability and use of the simulator two case study investigations will be carried out. The first of the case studies will be a theoretical investigation of the system $MgSO_4$-$H_2O$. The other case study will be of an industrial problem of a magnesium producing company, NEDMAG.

### 4.1 Case Study 1

Magnesium and sulphate ions are among the most common ions found in natural ground waters and aquatic environments (Archer and Rard, 1998). Creating a comprehensive solubility model of the system $MgSO_4$ - $H_2O$ based on its thermodynamic properties is difficult, not only because of the large number of crystalline hydrates occurring in the system, but also because of the strongly associative nature of the aqueous ions.

Recent interest has risen to recover magnesium sulphate heptahydrate ($MgSO_4.7H_2O$), for use as a fertilizer by crystallization from solutions of eutectic composition (Himawan *et al.*, 2002; Genceli *et al.*, 2003). $MgSO_4.12H_2O$ crystallizes at the eutectic and has to be subsequently converted to $MgSO_4.7H_2O$ by solution-mediated recrystallization. Therefore, detailed knowledge of the phase diagram in the system Mg-$SO_4$-$H_2O$ is needed. This can be achieved by simulation.

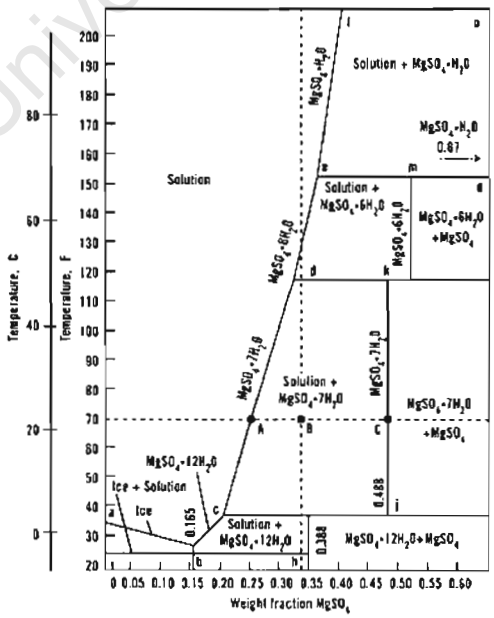


Figure 4.1: Phase diagram for $MgSO_4$-$H_2O$ system

Figure 4.1 shows the form of the diagram that is to be simulated. Of particular interest is the region defined by the weight fraction range 0 to 0.25 and temperature −10 to 5°C. In this region, there are three solid phases in existence viz. ice, epsomite ($MgSO_4.7H_2O$) and magnesium sulphate duodecahydrate ($MgSO_4.12H_2O$). Experimental solubility data for the $MgSO_4.12H_2O$ solid phase is scarce. This is because the phase exists at low temperatures and solubility measurements are difficult (Marion and Farren, 1999). The objective of this investigation is to use recently obtained experimental solubility data (Himawan, 2002) for this phase to model the solubility product and therefore to simulate its solubility line.

## 4.2 Case Study 2

### 4.2.1 Background of NEDMAG

NEDMAG is a producer of high-grade synthetic dead-burned magnesia and other magnesium compounds. This is achieved through solution mining of a mine in The Netherlands.

### 4.2.2 Solution Mining

Water is injected thus resulting in salt dissolution and the formation of caverns, which are large brine filled spaces. Impurities (such as clay) do not dissolve and thus this is an attractive process. Conversion of the salt from aqueous form to solid form is achieved by evaporation (crystallisation).

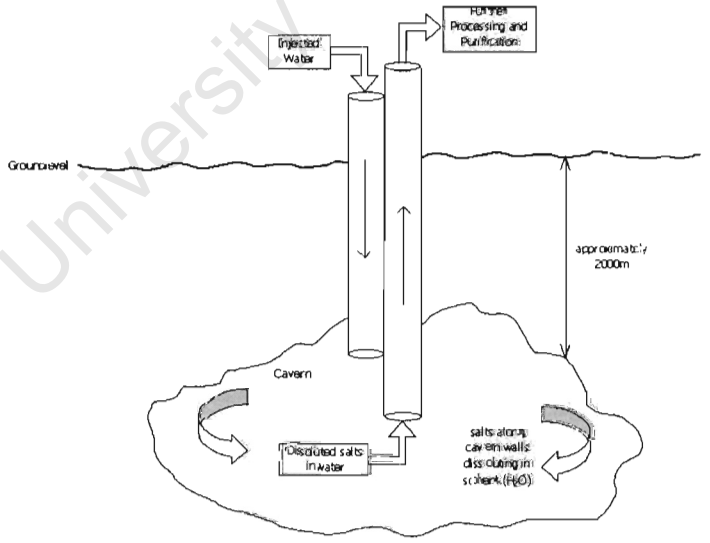


Figure 4.2: Diagram of solution mining

There are 8 caverns currently in operation at NEDMAG and the emphasis is on mining $MgCl_2$ from the caverns. The most common minerals (solid phases) evident in the caverns are sylvite (KCl), halite (NaCl), bischofite ($MgCl_2.6H_2O$) and carnallite ($KCl.MgCl_2.6H_2O$).

The brine exits the caverns above ground at a temperature of 55-60°C with an MgCl2 concentration of 33 to a maximum of 36 wt-%.

### 4.2.3 Problem

NaCl and KCl salts also occur in the caverns and these are dissolved into the brine. A recent examination of some of the brines exiting the caverns has revealed an increase in the concentration of NaCl and KCl over time. The average concentrations out of these caverns is 35 wt-% $MgCl_2$, 1.5 wt-% KCl and 1 wt-% NaCl.

Specifications limiting the allowable concentration of NaCl and KCl in the final product of NEDMAG require the lowering in concentration of the NaCl and KCl. At present the concentrations in most of the caverns still lie well below the maximum allowable concentration specifications of 0.2 wt-% and 0.4 wt-% for KCl and NaCl respectively. However, the forecast is that the remaining caverns will eventually exhibit the same trend with increasing concentrations. This means that some action is required in order to be able to make future use of the mines.

### 4.2.4 Possible Solution

It should be noted that these salts could be separated by different crystallisation methods. The KCl can be removed by cooling crystallisation, the NaCl by evaporative crystallisation and the Mg by precipitation. The process layout is dependant on a number of constraints such as the changing feed composition and the thermodynamics of the system.

A possible solution to the NEDMAG problem would be to design a process that would induce crystallisation. Of particular importance is that the crystals that forms are of minerals containing KCl and NaCl. In other words, it is desirable to reduce the concentration of these two by crystallising them out of solution. Cooling crystallisation could possibly be used to achieve this.

In order to examine the viability of a cooling crystallisation process, an examination of the phase diagram of the system can be used. In this particular case the phase diagram is ternary because there are three salts in the brines. At each temperature of interest a surface will exist to define the areas of existence of the minerals. Using the simulator this solubility diagram can be obtained. The temperature range of investigation will be from 0°C to 70°C.

# Chapter 5

# Details of Research Methods

## 5.1 Modelling Approach

In order to successfully develop a useful simulator, several decisions in the modelling process are required.

### 5.1.1 Choice of Model

The literature has shown that there are numerous approaches and models that describe the thermodynamic behaviour of electrolyte solutions. A decision about which of these to use is thus necessary.

The modelling approach of Pitzer has been found to best suit this investigation. The basis for this conclusion is that the Pitzer model provides good accuracy and applicability with relative simplicity. Further to this, the extended Pitzer models provide temperature dependency over a wide range and greater accuracy than other such models. This being the case the Pitzer parameters as proposed by Spencer et al. (1990) in conjunction with the revised sulphate parameters of Marion and Farren (1999) will be used in the simulator.

### 5.1.2 Choice of Software

The Pitzer equations are a system of non-linear equations that require simultaneous solution. In order to achieve this, mathematical modelling software will be used. The choice of appropriate software is based on literature research as well as the author's personal experience.

The criteria for ideal software for this investigation are:

- User friendly programming language
- User friendly debugger
- Reasonable computing power
- Possibility for adding greater complexity

The first two criteria are necessary to allow for ease of input of the programming language. A user-friendly debugger is essential in order to deal simply and efficiently with any convergence issues that may arise.

Mathematical modelling software packages that could be of use in this investigation are Matlab, g-PROMS and Polymath. Of these three, Polymath has the lowest computational power, in terms of solution convergence although it has a user-friendly interface and debugger.

Matlab and g-PROMS have good computational power and can both be extended to include more complexities. An example of such a complexity would be to use the simulator as a module in a process scheme in which it would act as an electrochemistry model. The rest of the process can be built around it and would probably include differential equations to account for balances on the process.

The g-PROMS debugger is more user friendly than that of Matlab. The programming involved in Matlab might require some extra programming knowledge. The solution of a system of non-linear equations in Matlab would require the use of one of Matlab's function functions such as fminsearch (Matlab, 2000). This would mean that the equations would have to be written in a specific format in order to get a solution.

The g-PROMS language is clear and concise and only allows the user to enter equations, as they would appear on paper (g-PROMS, 2002). This gives a user the freedom to concentrate on inputting the equations correctly instead of on solution techniques.

This user-friendly programming language means that g-PROMS can be passed on to other users with transparency.

The equations are presented here and are taken from Pitzer (1991).

### 5.1.3 The Pitzer Parameters

The parameters proposed by Spencer et al. (1990) in conjunction with the improved sulphate parameters determined by Marion and Farren (1999) will be used for low temperature prediction (<25°C). The parameters are functions of temperature and are represented by the equation:

$$P(T) = a_1 + a_2 \cdot T + a_3 \cdot T^2 + a_4 \cdot T^3 + a_5/T + a_6 \cdot \ln(T) \quad (5.1)$$

with T in K.

Table 5.1: Values of the fitting constants for the binary interaction parameters as functions of temperature for SMW model (Spencer et al., 1990) and FREZCHEM (Marion and Farren, 1999)

| Parameter | a1 | a2 | a3 | a4 | a5 | a6 |
|---|---|---|---|---|---|---|
| $\beta_{Na,Cl}^{(0)}$ | 7.872 | -8.39E-03 | 1.44E-05 | -8.78E-09 | -4.97E+02 | -8.21E-01 |
| $\beta_{Na,Cl}^{(1)}$ | 8.67E+02 | 6.06E-01 | -4.80E-04 | 1.89E-07 | -1.70E+04 | -1.67E+02 |
| $C_{Na,Cl}^{\phi}$ | 1.707 | 2.33E-03 | -2.47E-06 | 1.21E-09 | -1.355 | -3.87E-01 |
| $\beta_{Na,SO4}^{(0)}$ | -1.271 | 4.43E-03 | -3.50E-09 | -9.28E-10 | 1.43E+01 | -5.84E-03 |
| $\beta_{Na,SO4}^{(1)}$ | -1.3915 | 1.08E-02 | -1.83E-07 | -4.50E-09 | 9.33E+01 | -0.1678 |
| $C_{Na,SO4}^{\phi}$ | 0.2122 | -7.23E-04 | 0 | -1.14E-10 | 4.35 | -1.86E-03 |
| $\beta_{K,Cl}^{(0)}$ | 2.66E+01 | 9.93E-03 | -3.62E-06 | -6.28E-11 | -7.56E+02 | -4.673 |
| $\beta_{K,Cl}^{(1)}$ | 1.70E+03 | 1.223 | -9.99E-04 | 4.05E-07 | -3.29E+04 | -3.29E+02 |
| $C_{K,Cl}^{\phi}$ | -3.275 | -1.27E-03 | 4.71E-07 | 1.12E-11 | 9.08E+01 | 5.81E-01 |
| $\beta_{K,SO4}^{(0)}$ | -0.7568 | 2.53E-03 | 3.65E-08 | 5.31E-10 | -1.08 | -1.25E-03 |
| $\beta_{K,SO4}^{(1)}$ | 1.953 | -4.00E-03 | 3.55E-07 | 1.67E-08 | 2.67E+01 | -4.79E-02 |
| $C_{K,SO4}^{\phi}$ | 7.00E-04 | 4.80E-05 | 9.00E-09 | 3.26E-10 | -7.68 | 2.84E-03 |
| $\beta_{Ca,Cl}^{(0)}$ | -5.63E+01 | -3.01E-02 | 1.06E-05 | 3.33E-09 | 1.12E+03 | 1.07E+01 |
| $\beta_{Ca,Cl}^{(1)}$ | 3.478 | -1.54E-02 | 3.18E-05 | 0 | 0 | 0 |
| $C_{Ca,Cl}^{\phi}$ | 2.64E+01 | 2.47E-02 | -2.48E-05 | 1.22E-08 | -4.18E+02 | -5.354 |
| $\beta_{Ca,SO4}^{(0)}$ | 7.95E-02 | -1.22E-04 | 5.00E-06 | 6.70E-09 | -1.52E+02 | -6.89E-03 |
| $\beta_{Ca,SO4}^{(1)}$ | 2.89E+00 | 7.43E-03 | 5.29E-06 | -1.02E-07 | -2.08E+03 | 1.35E+00 |
| $C_{Ca,SO4}^{\phi}$ | 3.36E-02 | -1.53E-04 | 8.97E-07 | 1.57E-09 | 1.10E+00 | -1.28E-02 |
| $\beta_{Mg,Cl}^{(0)}$ | 3.14E+02 | 2.62E-01 | -2.46E-04 | 1.16E-07 | -5.53E+03 | -6.22E+01 |
| $\beta_{Mg,Cl}^{(1)}$ | -3.18E+04 | -2.87E+01 | 2.79E-02 | -1.33E-05 | 5.24E+05 | 6.41E+03 |
| $C_{Mg,Cl}^{\phi}$ | 5.95E-02 | -2.50E-04 | 2.42E-07 | 0 | 0 | 0 |
| $\beta_{Mg,SO4}^{(0)}$ | 1.68E+00 | -5.51E-03 | 5.97E-07 | 1.57E-08 | -2.24E+02 | 6.59E-02 |
| $\beta_{Mg,SO4}^{(1)}$ | 1.48E+00 | 6.27E-03 | 5.41E-06 | 8.84E-08 | -1.32E+03 | 0.3061 |
| $\beta_{Mg,SO4}^{(2)}$ | 1.88E+02 | -1.04E+00 | 1.22E-03 | 3.50E-06 | 8.98E+04 | -6.79E+01 |
| $C_{Mg,SO4}^{\phi}$ | 0.223 | -6.10E-04 | -1.00E-09 | -1.10E-09 | 4.27E+01 | -1.79E-02 |

The improved sulphate parameters as given by Marion and Farren (1999) are presented in Tables 5.1, 5.2 and 5.3 with the chloride parameters of Spencer et al. (1990). The original sulphate parameters of the SMW model are not reported here.

Table 5.2: Values of the fitting constants for the mixed salt parameters as functions of temperature for SMW model (Spencer et al., 1990) and FREZCHEM model (Marion and Farren, 1999)

| Parameter | a1 | a2 | a3 | a4 | a5 | a6 |
|---|---|---|---|---|---|---|
| $\theta_{Na,K}$ | -1.82E+01 | -3.69E-03 | - | 6.12E+02 | 3.029 | - |
| $\Psi_{Na,K,Cl}$ | 6.48 | 1.47E-03 | - | -2.04E+02 | -1.09 | - |
| $\Psi_{Na,K,SO4}$ | -5.63E-02 | 1.41E-03 | 2.30E-08 | -2.11E-08 | -2.57 | 1.85E-01 |
| $\theta_{Na,Ca}$ | 5.00E-02 | - | - | - | - | - |
| $\Psi_{Na,Ca,Cl}$ | -7.64 | -1.30E-02 | 1.11E-05 | - | 1.85 | - |
| $\Psi_{Na,Ca,SO4}$ | -8.08E-02 | 4.66E-03 | 5.55E-06 | -1.41E-07 | -1.09E+03 | 9.69E-01 |
| $\theta_{Na,Mg}$ | 7.00E-02 | - | - | - | - | - |
| $\Psi_{Na,Mg,Cl}$ | -3.11E-02 | 5.45E-05 | - | 1.99 | - | - |
| $\Psi_{Na,Mg,SO4}$ | -0.121 | 5.24E-04 | -5.39E-07 | -4.39E-10 | -1.72E+01 | 1.26E-02 |
| $\theta_{K,Ca}$ | 2.37 | -4.54E-03 | - | -2.85E+02 | - | - |
| $\Psi_{K,Ca,Cl}$ | -5.93E-02 | 2.54E-04 | 0 | -1.34E+01 | - | |
| $\theta_{K,Mg}$ | 1.17E-01 | - | - | - | - | - |
| $\Psi_{K,Mg,Cl}$ | 5.04E-02 | -8.75E-06 | - | -2.90E+01 | - | - |
| $\Psi_{K,Mg,SO4}$ | -0.118 | -4.78E-05 | -3.27E-07 | -9.37E-10 | 3.34E+01 | -8.84E-03 |
| $\theta_{Ca,Mg}$ | 5.31 | -6.34E-03 | - | -9.83E+02 | - | - |
| $\Psi_{Ca,Mg,Cl}$ | 4.16E+01 | 1.30E-02 | - | -9.82E+02 | -7.41 | - |
| $\theta_{Cl,SO4}$ | 7.00E-02 | - | - | - | - | - |
| $\Psi_{Cl,SO4,Na}$ | 2.55E-02 | -6.14E-05 | -9.00E-09 | 3.04E-10 | -8.90E-01 | -2.28E-03 |
| $\Psi_{Cl,SO4,K}$ | 6.08E-02 | -1.82E-04 | -2.15E-08 | -3.28E-10 | 5.22E+00 | -3.01E-03 |
| $\Psi_{Cl,SO4,Ca}$ | -2.63E-02 | -9.46E-05 | -3.13E-07 | -1.28E-09 | 2.94E+01 | -6.49E-03 |
| $\Psi_{Cl,SO4,Mg}$ | 5.87E-02 | -8.97E-05 | 4.70E-08 | 6.50E-11 | -2.41E+01 | 4.35E-03 |

Table 5.3: Values of the fitting constants for the solubility product parameters as functions of temperature for SMW model (Spencer et al., 1990) and FREZCHEM model (Marion and Farren, 1999)

| Parameter | a1 | a2 | a3 | a4 | a5 | a6 |
|---|---|---|---|---|---|---|
| ice | 7.88E+03 | 1.17E+01 | -1.71E-02 | 1.24E-05 | -9.33E+04 | -1.73E+03 |
| halite | 9.14E+03 | 8.22 | -8.13E-03 | 3.96E-03 | -1.54E+05 | -1.84E+03 |
| sylvite | -1.63E+03 | -1.52 | 1.45E-03 | -6.94E-07 | 2.26E+04 | 3.33E+02 |
| bischofite | 7.52E+02 | 1.18E-01 | - | - | -2.43E+04 | -1.22E+02 |
| carnallite | -4.46E+01 | 2.32E-01 | -7.15E-04 | 5.33E-07 | -4.25E+03 | 8.59 |
| epsomite | 3.96E+00 | - | - | - | -2.47E+03 | - |
| $MgSO_4.12H_2O$ | -2.96E+01 | 8.85E-02 | - | - | - | - |

The parameters in Table 5.3 give the temperature dependency of the solubility products of some salts important to this work. These parameters as described in the work by Spencer et al. (1990) and Marion and Farren (1999) were determined simultaneously as those parameters given in Tables 5.1 and 5.2.

The necessary debugging of the script was then carried out until reasonable solution convergence was obtained. The built-in solver of g-PROMS, MA28 was used. The simulator has been set up for a maximum number of 5000 iterations with the maximum number of iterations with no improvement set at 100. The relative accuracy has been set at 1e-5. Once the simulator is converging to the specifications, verification of the predictions will be necessary to ensure model accuracy.

## 5.2 Simulator Verification

In order to show that the model is applicable for the purposes of the investigation it is important to verify using independent experimental data from literature. This will also serve to show that the simulator can reproduce the results of Spencer et al. (1990) and Marion and Farren (1999) achieved in the SMW and FREZCHEM models.

The SMW and FREZCHEM models have been set up to focus on the low temperature region (<25°C). This means that prediction at higher temperatures is of lower accuracy (Spencer et al., 1989).

The temperature range of interest in the second case study is from 0 to 70°C. In verifying the simulator, an additional investigation will to be check the degree of inaccuracy i.e. whether the SMW and FREZCHEM parameters can still be used at higher temperatures. Running the simulator at high temperatures (>25°C) and comparing the predictions both graphically and numerically against available experimental data will serve to show this.

Spencer, Møller and Weare (1990) made use of a sigma value ($\sigma$) (defined by Equation 3.4) to demonstrate the quality of their predictions. In order to show the accuracy of the simulators predictions, this value will also be used in this work to provide some numerical verification.

In a further attempt at numerical verification, the degree of correlation between the experimental values and the simulator predicted values was calculated using the built in RSQ worksheet function in Microsoft Excel (Microsoft, 2000). The equation used is:

$$R^2 = \frac{n \cdot (\sum X \cdot Y) - (\sum X) \cdot (\sum Y)}{\sqrt{[n \cdot \sum X^2 - (\sum X)^2] \cdot [n \cdot \sum Y^2 - (\sum Y)^2]}} \qquad (5.2)$$

where n is the number of data points and X,Y represent the two data sets under examination

R is a dimensionless index ranging from –1 to 1. A value of 1 will mean exact correlation between the two data sets.

## 5.3 Methods for case studies

### 5.3.1 Case Study 1

Experimental Methods

The first case study required additional experimental solubility data. This was obtained in experiments run in the laboratories by Himawan (2002).

Experiments were conducted to determine the solubility of $MgSO_4.12H_2O$. Measurements were done in a 1-litre thermostated, jacketed glass vessel with a Teflon propeller-stirrer. Analytical Baker $MgSO_4.7H_2O$ with purity ± 99.9 wt-% and ultra-pure water of 18.2 MΩ were used. The following experimental procedure was followed:

- A carefully weighed solution (20.5 wt-% $MgSO_4$) was cooled down to below the eutectic temperature to crystallize out the $MgSO_4.12H_2O$ solid phase.

- The suspension was heated to the temperature at which the solubility was to be measured.

- The temperature was maintained for a minimum of 48 hours, to assure that the formation of the stable hydrate phase and the dissolution of any unstable phases was complete.

- Liquid samples were analysed for Mg and $SO_4$ using inductively coupled plasma spectrometry and ion chromatograph respectively.

The range of temperatures and compositions of interest are shown in Table 5.4. The table shows our data as well as other literature sources used in our model development.

Table 5.4: Experimental solubility data

| wt. % $MgSO_4$ | T(°C) | Solid phase | Reference |
|---|---|---|---|
| 8.90 | -1.48 | Ice | [1] |
| 12.74 | -2.15 | Ice | [1] |
| 14.97 | -3.00 | Ice | [1] |
| 18.00 | -3.90 | Ice | [1] |
| 20.57 | -5.20 | $MgSO_4.7H_2O$ | [2] |
| 21.26 | 0.00 | $MgSO_4.7H_2O$ | [1] |
| 21.38 | 1.80 | $MgSO_4.7H_2O$ | [1] |
| 23.25 | 10.00 | $MgSO_4.7H_2O$ | [1] |
| 24.29 | 12.60 | $MgSO_4.7H_2O$ | [1] |
| 24.41 | 15.00 | $MgSO_4.7H_2O$ | [1] |
| 25.20 | 20.00 | $MgSO_4.7H_2O$ | [1] |
| 26.25 | 20.00 | $MgSO_4.7H_2O$ | [1] |
| 26.70 | 25.00 | $MgSO_4.7H_2O$ | [1] |
| 26.90 | 25.00 | $MgSO_4.7H_2O$ | [1] |
| 28.02 | 29.89 | $MgSO_4.7H_2O$ | [1] |
| 29.30 | 35.00 | $MgSO_4.7H_2O$ | [1] |
| 30.80 | 40.00 | $MgSO_4.7H_2O$ | [1] |
| 32.30 | 45.00 | $MgSO_4.7H_2O$ | [1] |
| 33.00 | 48.00 | $MgSO_4.7H_2O$ | [1] |
| 33.40 | 50.00 | $MgSO_4.7H_2O$ | [1] |
| 16.77 | -3.87 | $MgSO_4.12H_2O$ | [2] |
| 17.12 | -3.74 | $MgSO_4.12H_2O$ | [2] |
| 18.07 | -2.80 | $MgSO_4.12H_2O$ | [2] |
| 17.87 | -3.43 | $MgSO_4.12H_2O$ | [2] |
| 17.59 | -3.72 | $MgSO_4.12H_2O$ | [2] |
| 18.72 | -2.00 | $MgSO_4.12H_2O$ | [2] |
| 19.87 | -1.33 | $MgSO_4.12H_2O$ | [2] |
| 20.21 | -0.30 | $MgSO_4.12H_2O$ | [2] |

[1] Linke and Seidell, 1965

[2] Himawan, 2002

Solubility Modelling

The solubility of a solid phase can be expressed thermodynamically by its solubility product, $K_{sp}$, the product of the activities of the dissolved species of the solid. The three solid phases in the region of investigation are ice, epsomite and magnesium sulphate duodecahydrate. For the Mg-$SO_4$-$H_2O$ system, the solubility products of ($MgSO_4.12H_2O$), ($MgSO_4.7H_2O$) and ice are defined as:

$$K_{sp,MgSO_4.7H_2O} = a_{Mg^{2+}} \cdot a_{SO_4^{2-}} \cdot a_w^7 \quad (5.3)$$

$$K_{sp,MgSO_4.12H_2O} = a_{Mg^{2+}} \cdot a_{SO_4^{2-}} \cdot a_w^{12} \quad (5.4)$$

$$K_{sp,ice} = a_w \quad (5.5)$$

where $a_i$ is the activity of the relevant ionic species.

In the modified Pitzer models of SMW and FREZCHEM, the $K_{sp}$ is written in the form of equation 5.1 where $a_i$ are tabulated parameters and T is the temperature in K.

There are expressions of this form for all the solid phases with the parameters and the temperature defining their solubility products (examples of these are given in Table 5.3). Marion and Farren (1999) proposed such an expression for the $MgSO_4.12H_2O$ solid phase for use in the FREZCHEM model. The emphasis of this work is on improving the prediction of the $MgSO_4.12H_2O$ solubility line by proposing an improved temperature dependant solubility product fit. The FREZCHEM model is applicable up to a maximum temperature of 25°C (Marion and Farren, 1999). An additional task for this investigation is to determine whether the applicability of the simulator can be extended with a temperature dependant solubility product fit that takes into account higher temperatures. Ultimately an improved phase diagram will be obtained.

The fit functions were obtained in the following way. Experimentally determined solubilities in the temperature range of -5 to 50°C were used for calculation of activity and osmotic coefficients with the FREZCHEM model, i.e. equations 3.1, 3.4 to 3.19. These were converted into activities of the ionic species and water from the molal concentrations. The activities were inserted in equations 5.3 to 5.5 for determination of the solubility products at various temperatures. The empirical equation 5.1 was fit to reproduce the so-obtained temperature

dependence of the solubility products. The FREZCHEM ion-interaction parameters were used without modification. With this approach, the framework of this widely applicable model remains unaltered, and improved solubility predictions in the Mg-$SO_4$-$H_2O$ system are derived.

These fits were then inputted at different temperatures into the g-PROMS simulator with the output being the predicted solubilities of the solid phase in question.

### 5.3.2 Case Study 2

The development of a cooling crystallisation process requires knowledge of the system phase diagram. The NEDMAG case is a ternary system (Mg-K-Na-Cl-$H_2O$ system) and therefore the resulting phase diagram will be 3-dimensional.

The Solid phases

An examination of recent brine samples shows that there are four possible solid phases that can be in existence in the system viz. sylvite (KCl), halite (NaCl), bischofite ($MgCl_2.6H_2O$) and carnallite ($KCl.MgCl_2.6H_2O$).

Using the $K_{sp}$ functions of these phases as proposed by Spencer et al. (1989), the simulator was used to calculate the solubilities of KCl, NaCl and $MgCl_2$ at which these phases exist. From these solubilities, the solubility surfaces of the four phases were determined. When comparing the surfaces, the minimum value at each temperature is a point for the system solubility surface. This means that at each temperature there will be a solubility surface. These surfaces are made up of the individual solubility surfaces of the solid phases.

By making use of these solubility surfaces, the necessary crystallisation route required to reduce the KCl and NaCl can be determined.

The 3-dimensional diagram

Figure 5.1a) is an example of the type of solubility surfaces expected at a specific temperature. On the x-axis, y-axis and z-axis are the weight percents of the three salts. Also shown in the Figure 5.1 are the different side-on views of the surface. The resulting lines shown in Figures 5.1b), c) and d) are obtained by making a cross section of the surface along the various axes. For instance Figure 5.1b), which is the NaCl-$MgCl_2$ face, is obtained when a cross section is made at 0 wt-% KCl. This is the solubility line on that face and this applies to all the other faces.

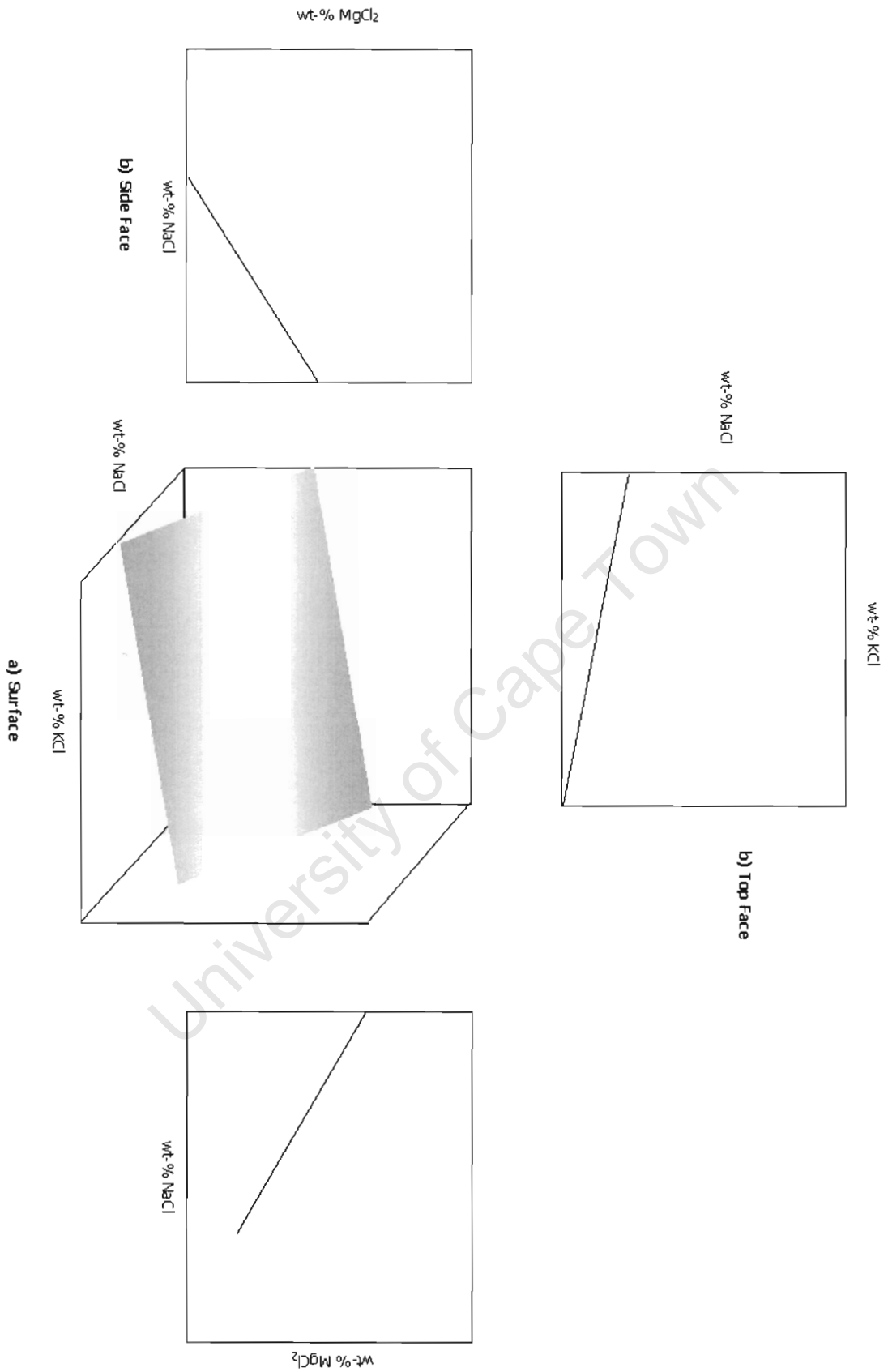




Figure 5.1: An example of the 3-dimensional diagram

# Chapter 6

## Results and Discussion

### 6.1 Simulator Verification

In order to show that the simulator can be applied to the systems of interest, simulator predictions of those systems and more specifically the solid phases that occur will be shown and interpreted here. The degree of inaccuracy for higher temperature predictions for these systems is also of particular interest for the second case study.

#### 6.1.1 Halite (NaCl)

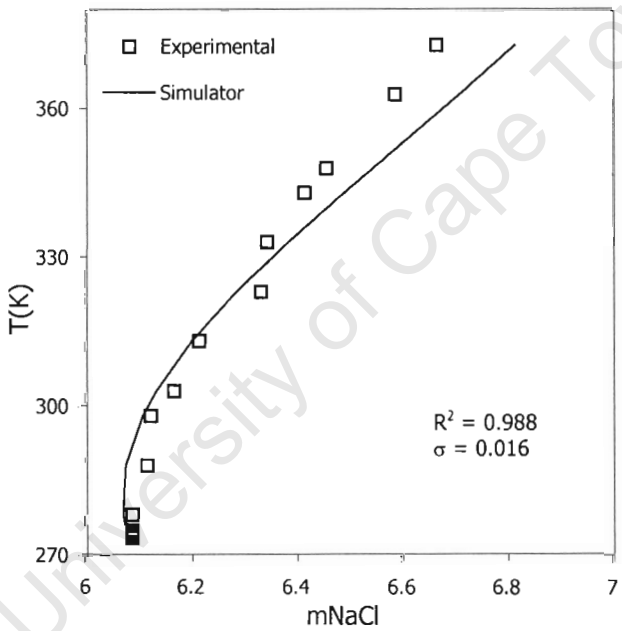




Figure 6.1: Predicted vs. experimental for the solubility line of halite (NaCl) over entire temperature range (Experimental data from Linke and Seidell (1965) and Liu and Lindsay (1972))

Figure 6.1 shows the solubility line for the solid phase halite (NaCl) over a wide temperature range (270 to 380K). Up to 27°C (~300K), the predictions of the simulator are in excellent agreement with experimental data. This is further supported by Figure 6.2 below, which shows a magnified view of the low temperature region. The predictions at higher temperatures show some deviation but this is expected. Even up to a temperature of 60°C (~330K) there is still good agreement. Above that temperature the prediction is less accurate. An $R^2$ value of 0.988 is a further indication of the accuracy of prediction. A low sigma value is further numerical evidence that the predictions are accurate.

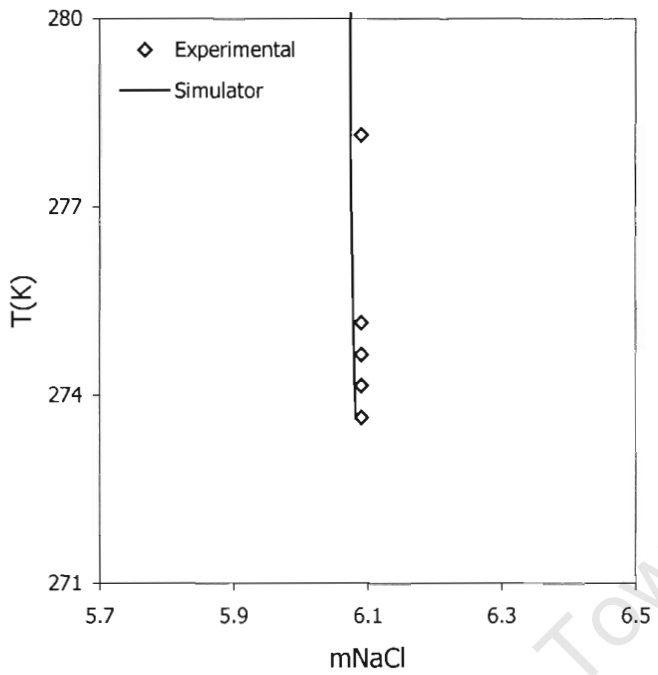


Figure 6.2: Predicted vs. experimental for the solubility line of halite (NaCl) over low temperature range

### 6.1.2 Sylvite (KCl)

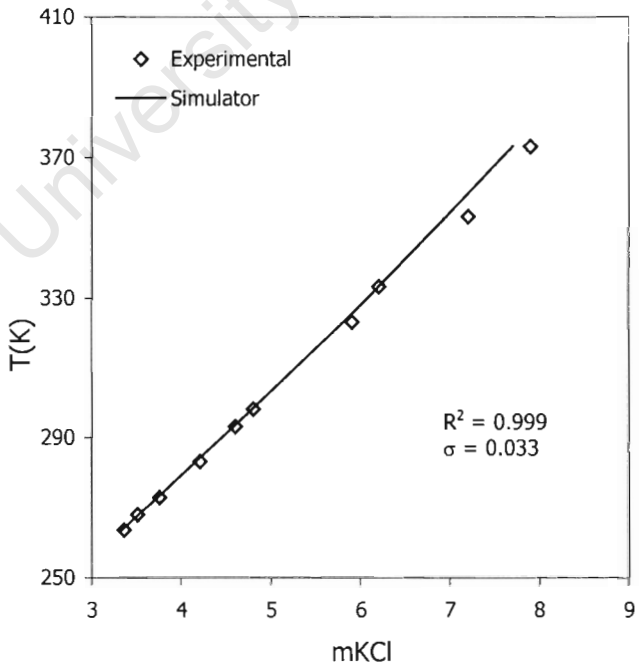


Figure 6.3: Predicted vs. experimental for the solubility line of sylvite (KCl) over entire temperature range (Experimental data from Linke and Seidell (1965))

The prediction for sylvite when compared against experimental data shows excellent agreement even at higher temperatures though there is some deviation observed. The $R^2$ value of 0.999 clearly shows that there is excellent correlation between the experimental and predicted data. A $\sigma$ value of 0.033 is low indicating that the predictions are not far from experimental data.

### 6.1.3 Bischofite ($MgCl_26H_2O$)

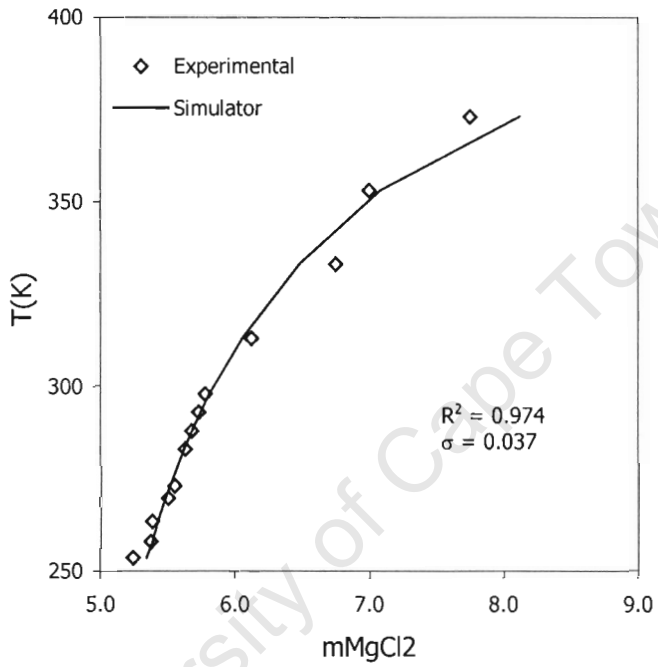


Figure 6.4: Predicted vs. experimental for the solubility line of bischofite ($MgCl_2.6H_2O$) over entire temperature range (Experimental data from Linke and Seidell (1965))

The results for the $MgCl_2$ system can be observed in Figure 6.4. The predicted values follow the trend of the experimental data for the entire temperature range. The lower temperature predictions are in excellent agreement with the experimental data. At higher temperatures deviation is again observed. The $R^2$ value indicates that correlation is least accurate for this solid phase although a value of 0.974 is reasonably good. A $\sigma$ value of 0.033 is also reasonably low indicating that the predictions are not that far from experimental data.

### 6.1.3 Carnallite ($KCl.MgCl_2.6H_2O$)

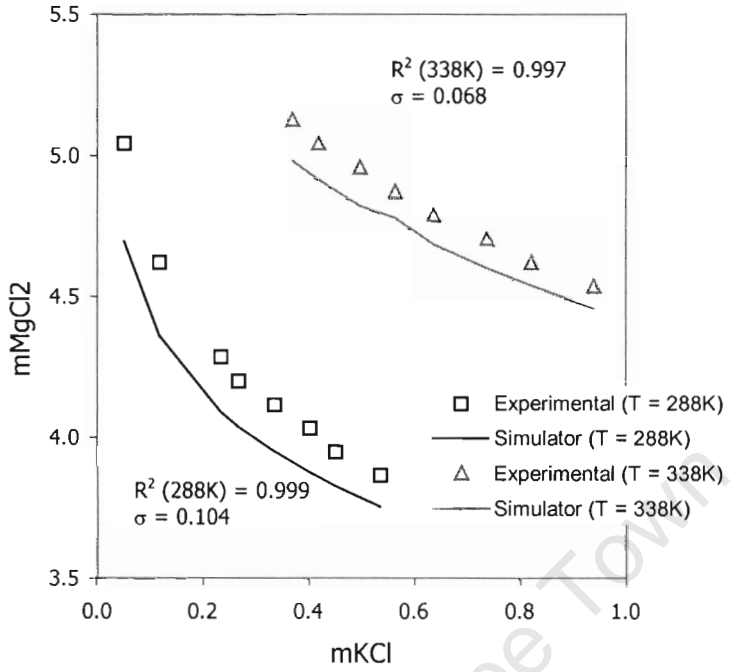


Figure 6.5: Predicted vs. experimental for the solubility line of carnallite ($KCl.MgCl_2.6H_2O$) over entire temperature range (Experimental data from Linke and Seidell (1965))

Figure 6.5 differs from previous figures that have been presented in that the axes represent the concentration of each of the two salts. The curves represent the solubility of carnallite at different temperatures. The predictions are in good agreement with the experimental data. As can be seen in Figure 6.5, the correct trend is predicted. In comparison to the figures already presented the results shown on this figure seem the least accurate. The scale on the y-axis means that a misleading visual examination is given.

An examination of the $R^2$ values however provides the proper perspective. The $R^2$ values of 0.999 and 0.997 for the different temperatures show that the predictions are excellent. The higher temperature $R^2$ is lower but it is expected that the higher temperature predictions are less accurate. The $\sigma$ values of 0.104 and 0.068 are reasonably low and are further indicators of the quality of prediction. Carnallite ($KCl.MgCl_2.6H_2O$) exists in a multi-component mixture of KCl and $MgCl_2$ therefore this also serves to illustrate that solubilities for multi-component mixtures are also accurately predicted by the simulator.

Deviations from the experimental data have been shown graphically and numerically for all of the four phases. The simulator has predicted the solubility lines for the phases with excellent accuracy. Therefore, the deviations observed at higher temperatures are not significant enough to disregard using the simulator for the second case study.

## 6.2 Case Study 1

### 6.2.1 The ice line

The $K_{sp}$ versus T dependency originally proposed in the FREZCHEM model follows equation 5.21 with the parameters shown in Table 5.3. The correlation results in a prediction that corresponds satisfactorily to experimental measurements. This is observed in Figure 6.6. Therefore, no refinement of the ice line was applied in this work.

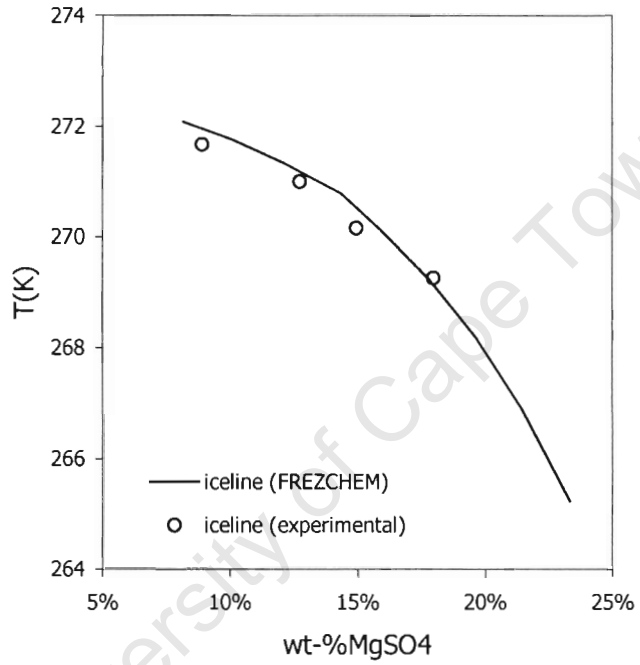


Figure 6.6: Prediction of the ice line in comparison to experimental data (Linke and Seidell, 1965)

The ice line predicted by the FREZCHEM model was verified not only against the experimental data of Himawan (2002), but also against vapour pressure data of ice and super-cooled water given by Mason (1971) and Gibbs free enthalpy data of freezing given by Leyendekkers et al. (1985). The ice line prediction of the FREZCHEM model matches the ones obtained from these data sets excellently and the FREZCHEM ice line was used unaltered in this simulator.

## 6.2.2 The Salt lines

For comparison, the correlations used in the FREZCHEM model and those proposed in this work are shown in Table 6.1. Both correlations are expressions of the form of equation 5.21.

Table 6.1: Comparison of the fit parameters for Ln(Ksp) of the solid phases

| $Ln(K_{sp})$ | a1 | a2 | a3 | a4 | a5 | a6 | $R^2$ |
|---|---|---|---|---|---|---|---|
| *FREZCHEM* | | | | | | | |
| $MgSO_4.7H_2O$ | 3.96 | - | - | - | -2.47E+03 | - | - |
| $MgSO_4.12H_2O$ | -29.58 | 0.089 | - | - | - | - | - |
| *This work* | | | | | | | |
| $MgSO_4.7H_2O$ | -32.03 | 0.165 | -2.42E-04 | - | - | - | 0.996 |
| $MgSO_4.12H_2O$ | -30.62 | 0.093 | - | - | - | - | 0.951 |

The $R^2$ value of the fit is also given in the table. It is a useful statistical evaluation of the quality of the fit in comparison to the calculated solubility products. The $R^2$ value of the FREZCHEM fit was not reported and the experimental data used is also not available. Thus statistical comparison is not possible.



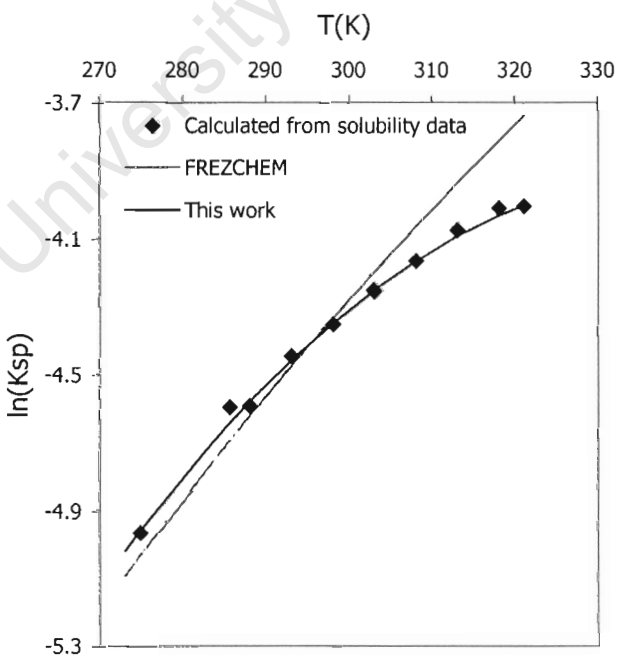


Figure 6.7: $Ln(K_{sp})$ vs. T for $MgSO_4.7H_2O$

Figure 6.7 shows that the proposed correlations for the $MgSO_4.7H_2O$ solid phase gives predictions that compare well with their respective calculated solubility products.

For $MgSO_4.7H_2O$ the data used by Marion and Farren (1999) for the FREZCHEM model is restricted to a narrower temperature range (0 to +25 °C) than the data used in this work (-5 to +50 °C). Figure 6.7 also shows that the FREZCHEM correlation does not extrapolate correctly for temperatures above 25 °C as opposed to the correlation of this work, which extrapolates well to higher temperatures.

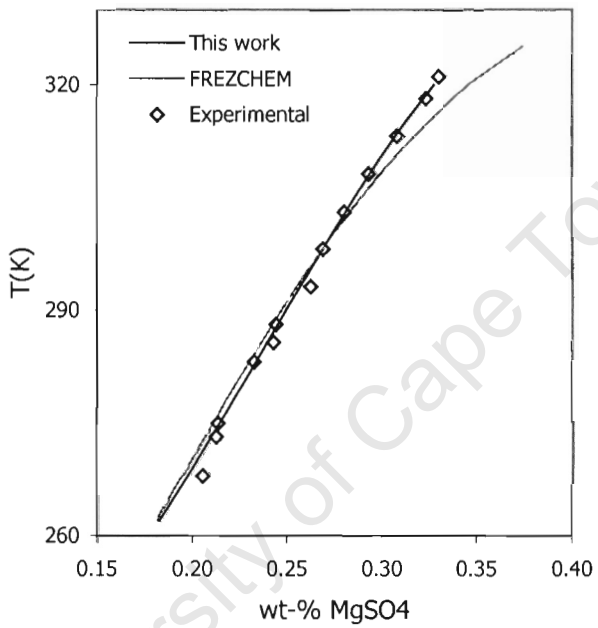




Figure 6.8: Comparison of solubility line predictions for $MgSO_4.7H_2O$ solid phase (Experimental data from Linke and Seidell (1965))

Figure 6.8 provides further evidence of the improvement of the correlation. It shows the predicted solubility lines for the solid phase in comparison with each other and with the experimental data. At temperatures greater than 25°C, the FREZCHEM prediction deviates from the experimental data. At temperatures below 25°C, there is no difference in the predicted solubility lines. The prediction from this work represents the experimental data more accurately at temperatures greater than 25°C.

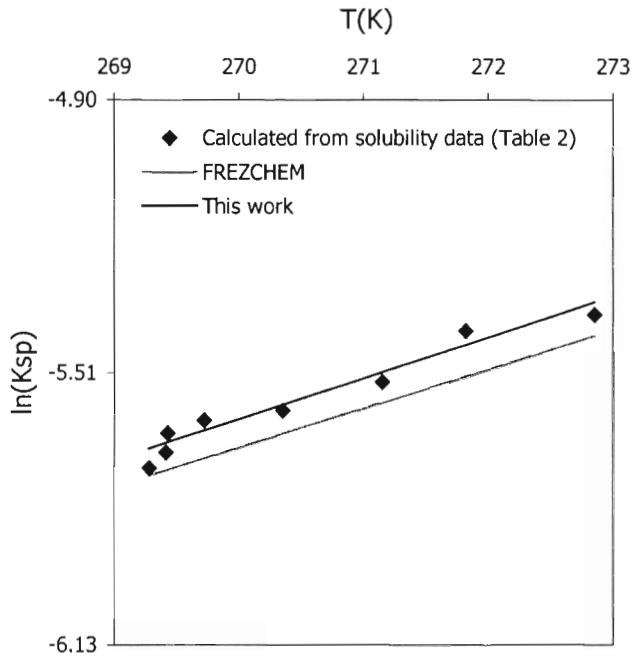


Figure 6.9: Ln($K_{sp}$) vs. T for $MgSO_4.12H_2O$

The correlations for $MgSO_4.12H_2O$ can be observed in Figure 6.9. The FREZCHEM correlation for $MgSO_4.12H_2O$ yields a fit that lies below our measurements, probably because the experimental data (Bukshtein et al., 1953) used is less reliable. Marion and Farren (1999) acknowledge that their estimate was based on scarce data and that hydrates of magnesium sulphate recrystallize slowly, making interpretation of experimental data difficult.

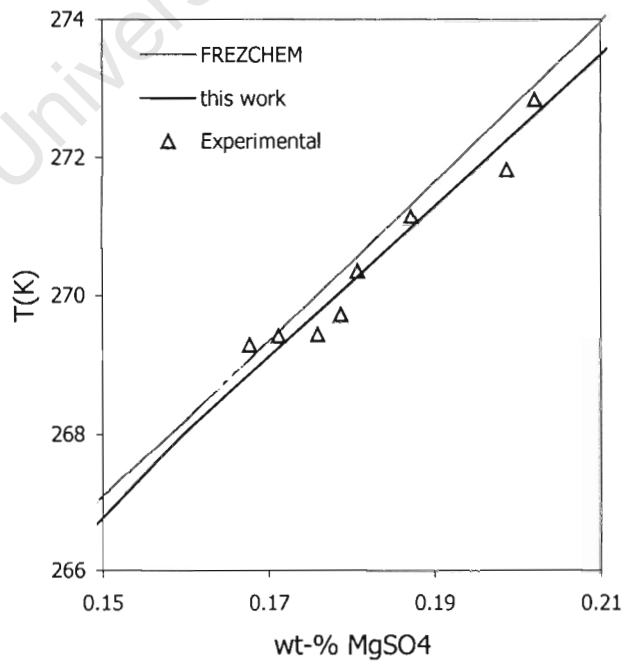


Figure 6.10: Comparison of solubility line predictions for $MgSO_4.12H_2O$ solid phase

In Figure 6.10, a direct comparison between the predicted solubility lines of the FREZCHEM model, the simulator of this work and the experimental data is carried out. Both the predictions follow the trend of the experimental data but the solubility line predicted in this work is in better agreement.

### 6.2.3 Salt lines and ice line: The phase diagram

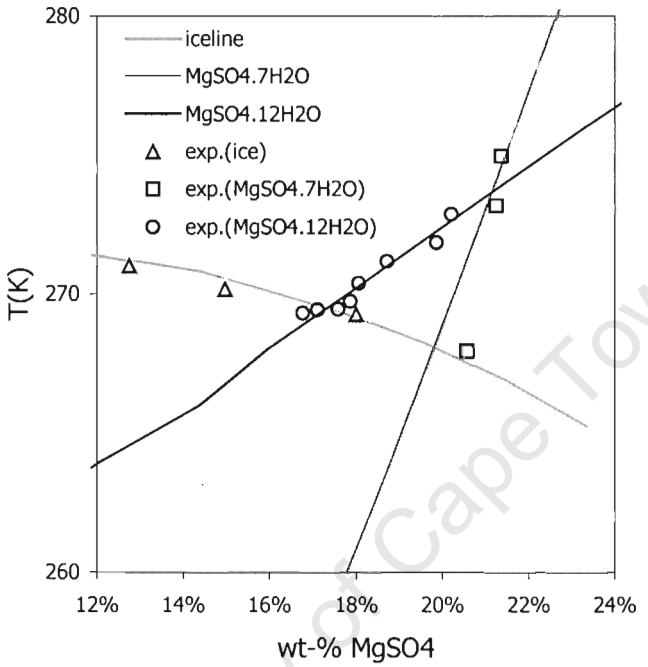


Figure 6.11: Predicted phase diagram of the system $MgSO_4$-$H_2O$ at eutectic conditions

Figure 6.11 shows experimental and calculated solubility lines and the ice line for conditions around the eutectic point. It was found in the experiments of Himawan (2002) that the eutectic point of the system is at 17.4 wt-% $MgSO_4$ and -3.7 °C. The simulator predicts the eutectic as 17.3 wt-% $MgSO_4$ and -3.7 °C. The FREZCHEM model predicted the eutectic at 17.3 wt-% $MgSO_4$ and -3.6 °C.

It can be noted that there is a deviant point in the experimental data of Figure 6.11 that occurs at approximately 20.5 wt-% $MgSO_4$ and -5.15 °C. It is most probably the meta-stable eutectic point of epsomite-ice that has been measured here. The simulator prediction is 19.7 wt% and -5.2°C and the FREZCHEM model predicts 19.6 wt-% and -5.0°C.

Linke and Seidell (1965) gave a eutectic point for epsomite ($MgSO_4.7H_2O$) - ice as 17.0 wt-% and -3.5°C. It appears that they misidentified the duodecahydrate as heptahydrate. The transition point between epsomite and the duodecahydrate phase is predicted as being at 21.1 wt-% $MgSO_4$ and 0.55°C. The FREZCHEM prediction is 21.8 wt-% $MgSO_4$ and 0.61°C.

The above results show that the simulator accurately describes the solubility lines of the $MgSO_4$-$H_2O$ system. In addition it predicts the two eutectics and the peritectic of the system. It is more accurate than the FREZCHEM model for epsomite for temperatures above 25°C. It is also more reliable and accurate for magnesium sulphate duodecahydrate.

## 6.3 Case Study 2

It has been shown that the simulator accurately predicts the solid phases halite (NaCl), sylvite (KCl) and bischofite ($MgCl_2.6H_2O$) and carnallite ($KCl.MgCl_2.6H_2O$). It was also observed that predictions for multi-component systems are accurate. Therefore the simulator can be applied to the second case study.

### 6.3.1 2-Dimensional vs. 3-Dimensional

Examining two-dimensional versions of a solubility diagram is a useful exercise but it is limited. Figures 6.12 and 6.13 presented below are two-dimensional views of the KCl-NaCl-$MgCl_2$-$H_2O$ system. These figures were obtained from NEDMAG. The axes of Figure 6.12 are the weight percentages of KCl and $MgCl_2$, while the axes of Figure 6.13 are the weight percentages of NaCl and $MgCl_2$. Specified on the figures are the regions of existence for the different solid phases.

These figures can be used in the development of the process to remove the KCl and NaCl. The problem though is that the weight percent of one component affects that of another. This means that in removing one component the weight percent of the others changes as well. As a means of illustration, consider Figure 6.12 and the initial concentrations of the brine, which is also shown in the figure. A temperature reduction will cause the concentration of $MgSO_4$ to decrease until the bischofite-carnallite equilibrium line is reached. This means that these two solid phases will crystallise along this line. The formation of carnallite is desirable since the decrease in KCl concentration is to be achieved in this way.

This approach is not quite correct since there is another component in the system. By looking at this face only, the NaCl is being neglected. The temperature reduction will affect the concentration of NaCl and this will in turn affect the concentrations of the other two components thus affecting where the equilibrium lines will lie. Therefore a 3-dimensional diagram will be of more use because it will provide the correct perspective of the system and illustrate how changes in one component can affect another.

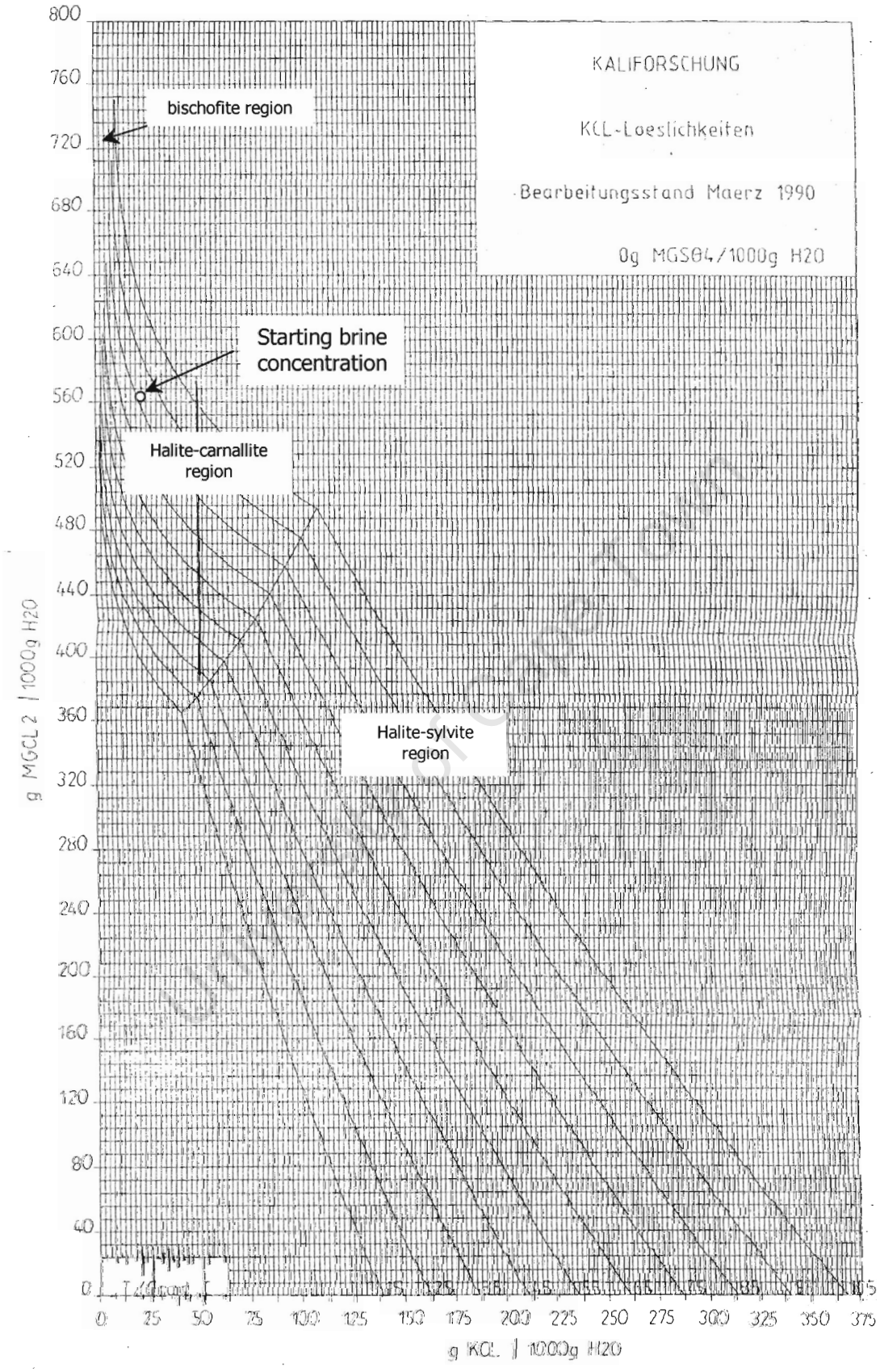


Figure 6.12: Solubility lines on the KCl-$MgCl_2$ face

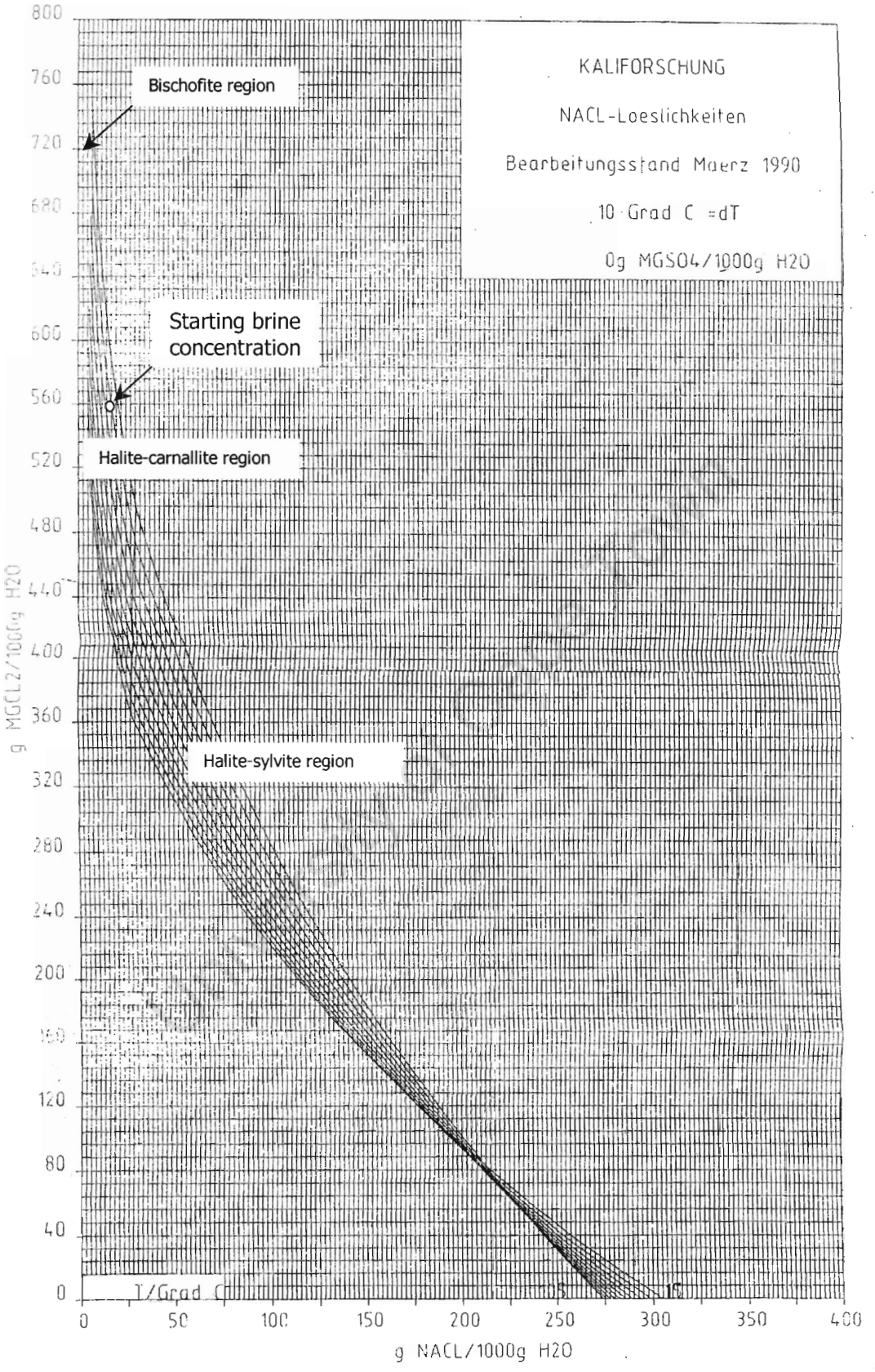


Figure 6.13: Solubility lines on the NaCl-$MgCl_2$ face

## 6.3.2 The Solubility Surfaces

The predicted 3-dimensional surfaces are presented here with some discussion around their use for the case study.

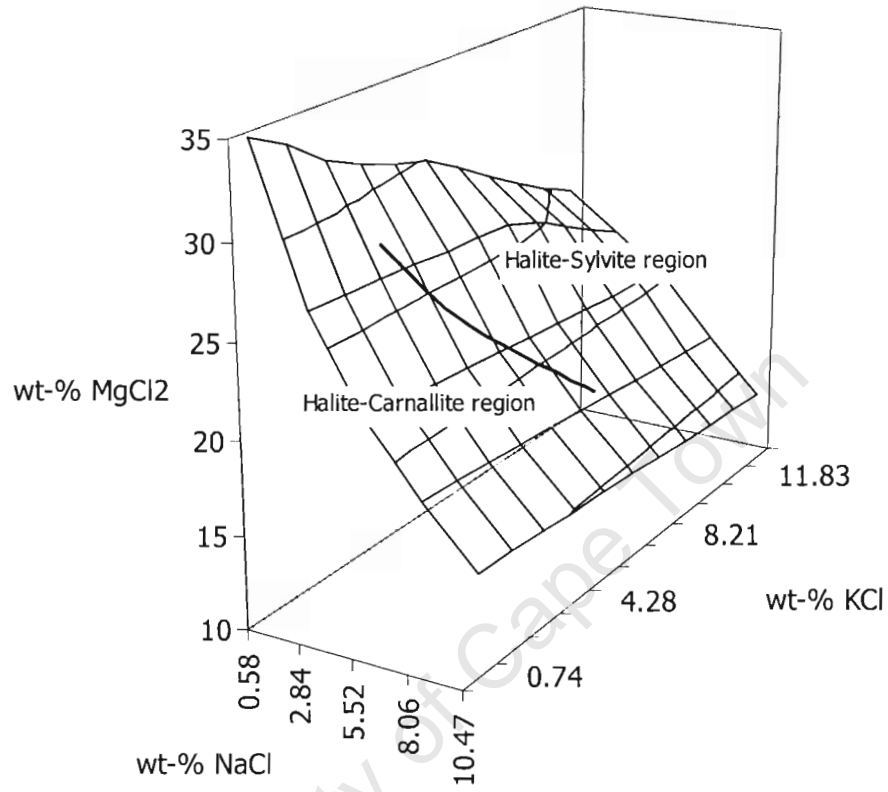


Figure 6.14: 3-dimensional solubility surface for 333K (60°C)

Table 6.2: Data used to plot the surface at a temperature of 333K (60°C) (Values are in wt-%)

| 333K (60°C) mKCl/mNaCl | 0.58 | 2.84 | 5.52 | 8.06 | 10.47 |
|---|---|---|---|---|---|
| 0.74 | 34.71 | 26.67 | 21.81 | 18.28 | 15.37 |
| 1.47 | 33.69 | 26.61 | 21.73 | 18.19 | 15.29 |
| 2.90 | 32.11 | 26.48 | 21.58 | 18.03 | 15.13 |
| 4.28 | 31.14 | 26.36 | 21.43 | 17.87 | 14.97 |
| 5.63 | 30.42 | 26.23 | 21.28 | 17.72 | 14.81 |
| 6.94 | 29.83 | 26.11 | 21.13 | 17.56 | 14.66 |
| 8.21 | 28.70 | 25.99 | 20.98 | 17.40 | 14.50 |
| 9.45 | 27.44 | 25.32 | 20.84 | 17.25 | 14.35 |
| 10.66 | 26.30 | 24.24 | 20.69 | 17.10 | 14.20 |
| 11.83 | 25.25 | 23.24 | 20.55 | 16.95 | 14.05 |
| 12.98 | 24.26 | 22.30 | 20.17 | 16.80 | 13.90 |

KCl
NaCl
$MgCl_2.6H2O$
$KCl.MgCl_2.6H2O$

Figure 6.14 is the solubility surface for a temperature of 333K. In Figure 6.15, the solubility surfaces at lower temperatures are observed to have a similar shape lying below the surface presented in Figure 6.14.

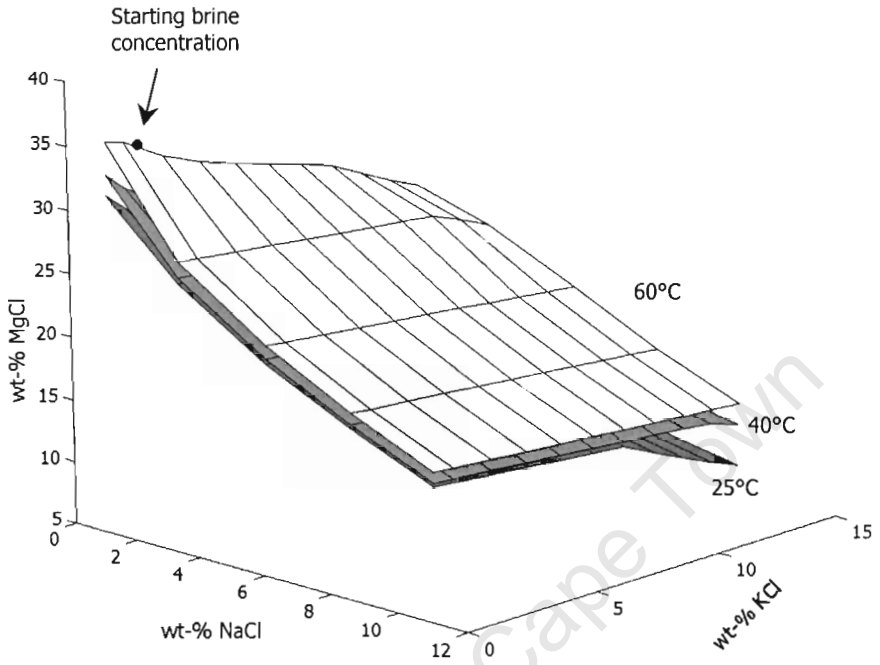


Figure 6.15: 3-dimensional solubility surface for 333K (60°C)

The brine concentration as provided by NEDMAG is 35 wt-% $MgCl_2$, 1.5 wt-% KCl and 1 wt-% NaCl. This is illustrated in Figure 6.15.

The data points used to plot the surface of Figure 6.14 are given in Table 6.2. Similar tables giving the data points for different temperatures can be found in Appendix C. These values are the minimum solubility values for the different solid phases. Different shadings have been used to show the apparent solid phases present at the respective data points. It is important to note in this table is that there is no $MgCl_2.6H_2O$ region. The reason for this is that the $MgCl_2.6H_2O$ region is a small region and it exists only at very small concentrations of KCl and NaCl.

Further proof of this is in Figures 6.12 and 6.13, where the small $MgCl_2.6H_2O$ region can be clearly seen. The simulator has predicted that none of the $MgCl_2.6H_2O$ solubilities are the minimum solubilities of the system for the region of investigation. The inaccuracies for higher temperature prediction, especially for $MgCl_2.6H_2O$ mean that there is the possibility of error in the prediction of the solubilities of this phase.

A sigma value for the low temperature data points (253 to 298 K) is 0.00177 in comparison to a sigma value of 0.055 for the high temperature data points (313 to 373 K). The deviation from the experimental data could be significant in making up the surfaces. These uncertainties cast some doubt on how far the simulator in its current form can be used to design the crystallisation process. Nevertheless, the surfaces can still provide an indication of whether or not an appropriate crystallisation pathway can be determined.

Using the 3-dimensional surfaces in conjunction with the 2-dimensional faces shows that a reduction in temperature will move the concentrations of the three components onto an equilibrium surface such as the 60°C surface. The crystallisation route required would be in a direction so as to reduce the KCl and NaCl concentrations. At its current concentrations, the formation of $KCl.MgCl_2.6H_2O$ and NaCl is favoured with a reduction in temperature because the concentrations will move towards an equilibrium surface. This means that the KCl and NaCl concentrations will be reduced because they will crystallise out as $KCl.MgCl_2.6H_2O$ and NaCl respectively.

Some of the $MgCl_2$ will be lost as $KCl.MgCl_2.6H_2O$ but in the final design of the crystallisation process one of the main aims would be to reduce this loss while maximising the loss of KCl. The ultimate point of operation will be on an equilibrium line on one of the temperature dependant surfaces i.e. operation at a temperature such that the crystallisation of carnallite and halite is favoured. Figure 6.16 is a diagrammatic representation of the steps in the crystallisation. The figure shows the path on one surface i.e. for one temperature. Further cooling steps might be required in the final process.

Figure 6.16a shows the starting point with the feed conditions. Thereafter cooling will result in the solubility surface being reached. This is represented by Figure 6.16b. Figure 6.16c represents the effects of further cooling. From the feed composition at the top surface (at 60°C) the point representing the product mother liquor is reached.

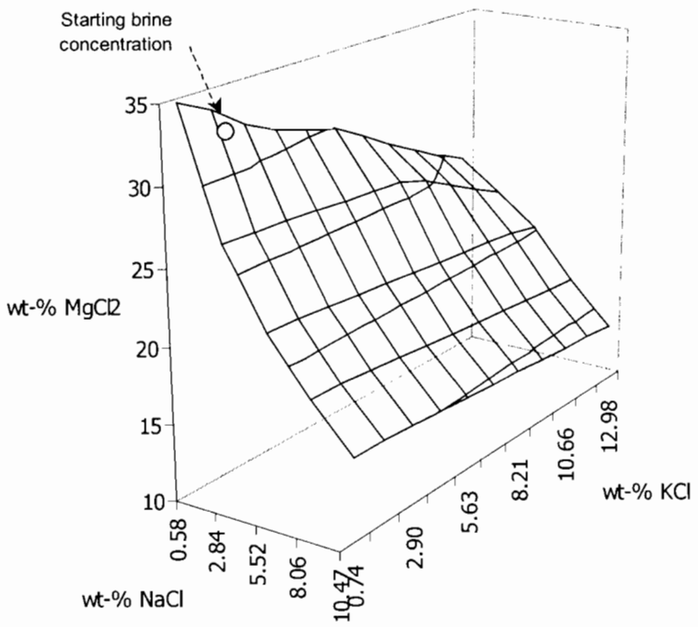


**a) Starting point**

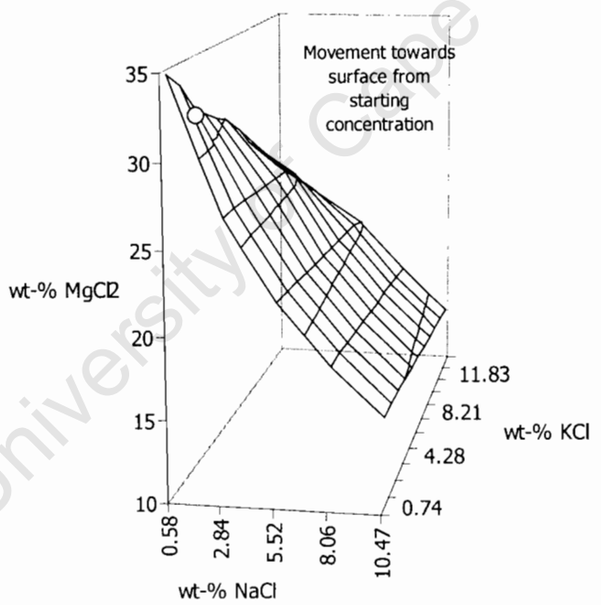


**b) reaching a surface**

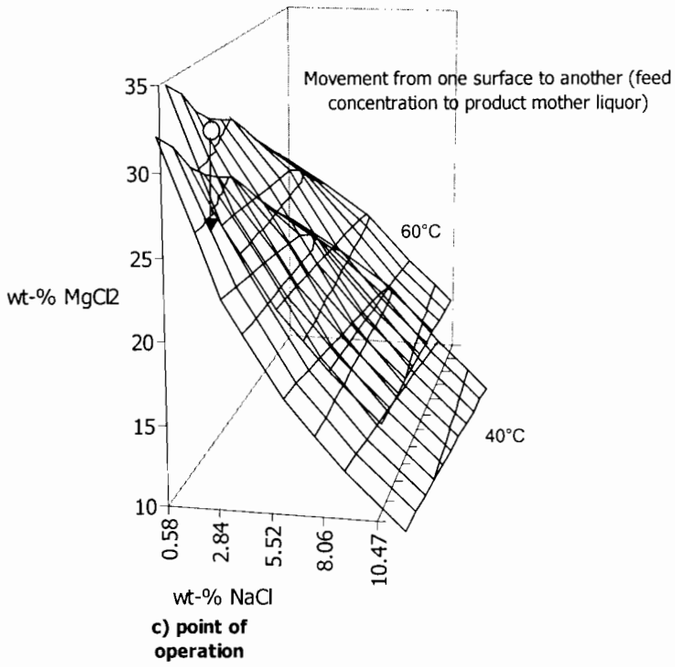


Figure 6.16 Representation of the crystallisation route (reaching equilibrium)

Further considerations of the feed concentrations reveal that it is at the NaCl/KCl.$MgCl_2$.$H_2O$ eutectic therefore cooling crystallisation will result in a product with a mix of both salts. This has been alluded to earlier. In essence this is a complicated system with many issues to consider before a final process can be determined.

The closeness of the feed concentrations to this eutectic point mean that an optimum separation process can only be designed with an accurate knowledge of the thermodynamics of the system.

# Chapter 7

## Conclusions

From the results presented here the following conclusions have been made:

- An equilibrium thermodynamic simulator that accurately describes the system K-Na-Mg-Cl-$SO_4$-$H_2O$ has been set up using the Pitzer framework, the semi-empirical parameters proposed by Spencer et al. (1990) and the revised sulphate parameters of Marion and Farren (1999);

- Although the original parameters used in the model are specifically for low temperature simulation, it has been found that high temperature predictions are reasonable;

- A correlation to describe the temperature dependence of the solubility product of $MgSO_4.7H_2O$ to increase its accuracy at higher temperatures has been proposed. This correlation improves the higher temperature prediction of the epsomite solubility line;

- Based on new solubility data a correlation to describe the temperature dependence of the solubility product of $MgSO_4.12H_2O$ has been proposed. Better predictions of the experimental data are obtained with this correlation than with the original FREZCHEM correlations;

- The potential for reducing the concentrations of KCl and NaCl from the NEDMAG brines has been confirmed with the aid of 3-dimensional diagrams describing the solubility surfaces of the system K-Na-Mg-Cl-$H_2O$, which have been developed with data obtained from the simulator.

- The closeness of the feed concentrations to the NaCl/KCl.$MgCl_2$.$H_2O$ eutectic point adds greater complexity to the problem meaning that an optimum separation process can only be designed with an accurate knowledge of the thermodynamics of the system.

## Future Work

Future work that could be carried out to build on the results and conclusions from this work are:

- The designing of the process to convert $MgSO_4.12H_2O$ to $MgSO_4.7H_2O$ by further computer simulation. The simulator has the potential to be of some use here because it could serve as the electrochemistry model in the process scheme.

- The inclusion of high temperature parameters (such as those proposed by Pitzer and Pabalan, 1987) by further programming to increase the usefulness of the simulator. Although the simulator in current form has been shown to be reasonably accurate at high temperatures, there is a limit to its value. These limitations were evident during the work carried out for the second case study.

- With a simulator able to make better high temperature predictions, the process scheme for the NEDMAG case study can be further investigated and the actual equilibrium lines could possibly be determined.

- Estimation of self-consistent ion interaction parameters over a wide temperature range. The SMW and FREZCHEM models focus specifically on estimating parameters for the low temperature region and there has been much work done on parameter estimation in the high temperature region (Pitzer and Pabalan, 1987; Møller, 1988; Greenberg and Møller, 1989). There is thus an opportunity to develop a model that incorporates a wide temperature range.

# References


Archer, D.G. and Rard, J.A. (1998) Isopiestic Investigation of the Osmotic and Activity Coefficients of Aqueous $MgSO_4$ and the solubility of MgSO4·7H2O(cr) at 298.15K: Thermodynamic Properties of the MgSO4 + H2O System to 440K. *J. Chem. Eng. Data* 43, 791-806

Aspen Plus Electrolyte Manual (1994) Aspen Technology, Inc., Cambridge

Ball, F.X., Fürst, W. and Renon, H. (1985a) An NRTL model for representation and prediction of deviation from ideality in electrolyte solutions compared to the models of Chen (1982) and Pitzer (1973). *AIChE J.*, **31**, 392-399

Ball, F.X., Fürst, W. and Renon, H. (1985b) Representation of Deviation from Ideality of Electrolytes using a Mean Spherical Approximation molecular model. *AIChE J.*, **31**, 1233-1240

Berthold, J. (2000) *A Guide to using the OLI Software*, OLI systems Inc.

Bromley, L.A. (1973) Thermodynamic Properties of Strong Electrolytes in Aqueous Solutions. *AIChE J.*, **19**, 313-320

Bukshtein, V.M., Valyashko, M.G., and Pel'sh, A.D. (eds.) (1953) *Spravochnik po rastvorimosti soleyvkh system.* Vols. I and II. Izd. Vses. Nauch.-Issled. Inst. Goz., Goskhimizdat., Moscow-Leningrad, 1270

Chen, C.C., Britt, H.I., Boston, J.F. and Evans, L.B. (1982) Local Composition Model for Excess Gibbs Energy of Electrolyte Systems. *AIChE J.*, **28**, 588-596

Chen, C.C., Evans, L.B., and Mock, B. (1986) Thermodynamic representation of Phase Equilibria of Mixed-Solvent Electrolyte Systems. *AIChE J.*, **32**, 1655-1664

Christov, C. (2001) Thermodynamic Study of the K-Mg-Al-Cl-$SO_4$-$H_2O$ system at the temperature 298.15 K. *Calphad*, **25**, 445-454

Cruz, J.L. and Renon, H. (1978) A new thermodynamic representation of binary Electrolyte Solutions non-ideality in the whole range of concentration. *AIChE J.*, **24**, 817-829

Genceli, E., Himawan, C., Seckler, M.M., Witkamp, G.J. (2003) Inline measurement of supersatutration in magnesium sulfate solutions by using conductivity and refractive index, will appear in the Proceedings of Workshop on Advance in Sensoring in Industrial Crystallization, June 18-20, 2003, Istanbul, Turkey

Gibbard, H.F. and Fong, S.L. (1975) Freezing points and related properties of electrolyte solutions III. The system NaCl-$CaC_{l2}$-$H_2O$ and NaCl-$BaCl_2$-H2O. *J. Sol. Chem.*, **4**, 863-872

Goldberg, R.N. (1981) Evaluated activity and osmotic coefficients for aqueous solutions: thirty-six uni-bivalent electrolytes. *J. Phys. Chem. Ref. Data* **10**, 671-764

g-PROMS Introductory Guide (2002) Process Systems Enterprise Ltd., London

Greenberg, J. and Möller, N. (1989) The prediction of mineral solubilities in natural waters: A chemical equilibrium model for the Na-K-Ca-Cl-$SO_4$-$H_2O$ system from 0°C to 250°C. *Geochim. Cosmochim. Acta*, **53**, 2503-2518

Gui-Wu, L., Chun-Xi, L., Ru, T., Zi-Hao, W., Wen-Chuan, W. (2004) Representation of the nonideality of electrolyte solutions using the cluster expansion theory. *Fluid Phase Equilibria*, **218**, 77-84

Hall, D.L., Sterner, S.M. and Bodnar, R.J. (1988) Freezing Point Depression of NaCl-KCl-$H_2O$ solutions. *Econ. Geol.*, **83**, 197-202

Harned, H.S. and Owen, B.B. (1958) *Physical Chemistry of Electrolyte Solutions*, 3rd ed., Reinhold

Harvie, C.E., Eugster, H. P., and Weare, J.H. (1982) Mineral equilibria in the six-component seawater system, Na-K-Mg-Ca-$SO_4$-Cl-$H_2O$ at 25°C. II: Compositions of the saturated solutions. *Geochim. Cosmochim. Acta*, **46**, 1603-1618

Harvie, C.E., Møller, N., and Weare, J.H. (1985) The prediction of mineral solubilities in natural waters: The Na-K-Mg-Ca-H-Cl-$SO_4$-OH-$HCO_3$-$CO_3$-$CO_2$-$H_2O$ system to high ionic strengths at 25°C. *Geochim. Cosmochim. Acta*, **48**, 723-751

Helgeson, H.C., Kirkham, D.H. and Flowers, G.C. (1974, 1976, 1981) Theoretical Prediction of the Thermodynamic Behaviour of Aqueous Electrolytes at High Pressures and Temperatures – Parts I – IV. *Amer. J. Sci.*

Himawan, C., Vaessen, R.J.C, Seckler, M.M., Witkamp, G.J. (2002) Recovery of magnesium sulfate and ice from magnesium sulfate industrial solution by eutectic freezing, In: Chemical Engineering Transactions, Volume 1, 2002. Proceedings of the 15th International Symposium on Industrial Crystallization, Sept. 15-18, 2002, Sorrento, Italy, pp. 951-956, ISBN 88-900775-0-6

Jin, G. and Donahue, M.D. (1988) An equation of state for electrolyte solutions. 1. Aqueous systems containing strong electrolytes. *Ind. Eng. Chem. Res.*, **27**, 1073-1084

Leyendekkers, J.V. and Hunter, R.J. (1985) Thermodynamic Properties of Water in the Subcooled Region I. *J. Chem. Phys* **82**, 1440-1446

Linke, W.F. and Seidell, A. (1965) *Solubilities of Inorganic and Metal-Organic Compounds: A Compilation of Solubility Data from Periodical Literature, Vol. II*, 4th ed., Van Nostrand

Liu, C. and Lindsay, W.T. JR. (1972) Thermodynamics of sodium chloride solutions at high temperatures, *J. Soln. Chem.* **1**, 45-69

Marion, G. (2001) Carbonate mineral solubility at low temperatures in the Na-K-Mg-Ca-H-Cl-$SO_4$-OH-$HCO_3$-$CO_3$-$CO_2$-$H_2O$ system. *Geochim. Cosmochim. Acta*, **65**, 1833-1896

Marion, G. (2002) A molal-based model for strong acid chemistry at low temperatures (<200 to 298 K). *Geochim. Cosmochim. Acta*, **66**, 2499-2516

Marion, G. and Farren, R.E. (1999) Mineral solubilities in the Na-K-Mg-Ca-Cl-$SO_4$-$H_2O$ system: A re-evaluation of the sulfate chemistry in the Spencer-Møller-Weare model. *Geochim. Cosmochim. Acta*, **63**, 1305-1318

Marion, G., Caitling, D.C. and Kargel, J.S. (2003) Modelling aqueous ferrous iron chemistry at low temperatures with application to Mars. *Geochim. Cosmochim. Acta*, **67**, 4251-4266

Matlab User Manual – Using Matlab version 6 (2000) The MathWorks, Inc.

Meissner, H.P. and Tester, J.W. (1972) Activity Coefficients of Strong Electrolytes in Aqueous Solutions. *Ind. Eng. Chem. Process Des. Develop.*, **11**, 128-133

Meissner, H.P., Kusik, C.L. and Tester, J.W. (1972) Activity Coefficients of Strong Electrolytes in Aqueous Solutions- Effect of Temperature. *AIChE J.*, **18**, 661-662

Microsoft Excel Help, Microsoft (2000)

Möller, N. (1988) The prediction of mineral solubilities in natural waters: a chemical model for the Na-Ca-Cl-$SO_4$-$H_2O$ system, to high temperature and concentrations. *Geochim. Cosmochim. Acta*, **52**, 821-837

Myers, J.A. and Sandler, S.I. (2002) An Equation of state for electrolyte solutions covering wide ranges of temperature, pressure and composition. *Ind. Eng. Chem. Res.,* **41**, 3282-3297

Pérez-Villaseñor, F., Iglesias-Silva, G.A. and Hall, K.R. (2002) Osmotic and Activity Coefficients using a Modified Pitzer Equation for strong electrolytes 1:1 and 1:2 at 298.15 K. *Ind. Eng. Chem. Res.*, **41**, 1031-1037

Pitzer, K. (1991) *Activity Coefficients in Electrolyte Solutions*, 2nd ed. CRC press

Pitzer, K. (1973) Thermodynamics of Electrolyte Solutions. I. Theoretical Basis and General Equations. *J. Phy. Chem.*, **77**, 268-277

Pitzer, K. and Kim, J.J. (1974) Thermodynamics of electrolytes IV. Activity and Osmotic Coefficients for Mixed Electrolytes. *J. Amer. Chem. Soc.*, **96**, 5701-5707

Pitzer, K. and Pabalan, R.T. (1987) Thermodynamics of concentrated electrolyte mixtures and the prediction of mineral solubilities to high temperatures for mixtures in the system Na-K-Mg-Cl-$SO_4$-OH-$H_2O$. *Geochim. Cosmochim. Acta*, **51**, 2429-2443

Planche, H. and Renon, H. (1981) Mean Spherical Approximation applied to a simple but non-primitive model of interaction for electrolyte solutions and polar substances. *J. Phy. Chem.*, **85**, 3924-3929

Renon, H. (1986) Electrolyte Solutions. *Fluid Phase Equilibria*, **30**, 181-195

Robinson, R.A. and Stokes, R.H. (1965) *Electrolyte Solutions*, 2nd ed., Academic Press

Sandler, S.I. (1994) *Models for thermodynamic and phase equilibria calculations*, Marcel Dekker, Inc.

Sandler, S.I. (1999) *Chemical and Engineering Thermodynamics*, 3rd ed. John Wiley and Sons, Inc.

Spencer R.J., Møller N., and Weare J.H. (1990) The prediction of mineral solubilities in natural waters. *Geochim. Cosmochim. Acta*, **54**, 575-590

Watanasiri, S. and Liu, Y. (1999) Successfully simulate electrolyte systems. *Chem. Eng. Prog.*, 25-41

Woods, J. R. (1975) Thermodynamics of brine-salt equilibriums I. The systems NaCl-KCl-$MgCl_2$-$CaCl_2$-$H_2O$ and NaCl-$MgSO_4$-$H_2O$ at 25°C. *Geochim. Cosmochim. Acta*, **39**, 1147-1163

Yanatieva, O.K. (1946) Polytherms of solubility of salts in the tropic system $CaCl_2$-$MgCl_2$-H2O and $CaCl_2$-NaCl-$H_2O$. *J. Appl. Chem.*, **19**, 709-722

# Appendix A – Miscellaneous Constants

A number of constants have been used in the simulator. They are reported in Table A-1.

Table A-1: Constants used in the simulator

| Constant | Value | Units |
|---|---|---|
| $\alpha_1$ | 2.0 | $kg^{0.5}/mol^{0.5}$ |
| $\alpha_1^*$ | 1.2 | $kg^{0.5}/mol^{0.5}$ |
| $\alpha_2$ | 1.4 | $kg^{0.5}/mol^{0.5}$ |
| b | 1.2 | $kg^{0.5}/mol^{0.5}$ |
| e | 1.6022E+19 | C |
| $\varepsilon_o$ | 8.8542E-12 | $C^2/J\ m$ |
| k | 1.3807E-23 | J/K |
| $N_A$ | 6.0221E+23 | particle/mol |
| $\Omega$ | 55.5 | mol/kg |
| R | 8.3144 | J/mol K |
| $U_1$ | 3.4279E+02 | K |
| $U_2$ | -5.0866E-03 | K |
| $U_3$ | 9.4690E-07 | K |
| $U_4$ | -2.0525 | K |
| $U_5$ | 3.1159E+03 | K |
| $U_6$ | -1.8289E+02 | K |
| $U_7$ | -8.0325E+03 | K |
| $U_8$ | 4.2142E+06 | K |
| $U_9$ | 2.1417 | K |

Note:

1. Most of the constants reported in the table are used for the calculation of the Debye-Hückel parameter using the method given in Pitzer (1991). The calculation of this parameter can also be achieved using correlations suggested by Marion and Farren (1999) for the FREZCHEM model.

2. The constant $\alpha_1$ has two reported values in the table. This is because this constant has a different value for 2-2 salts such as $MgCl_2$. The second reported value is used together with $\alpha_1$ denoted with * for 2-2 salts.

# Appendix B – Script Files

The script files used in the simulator are reported here. g-PROMS has a main PROCESS script file from which other MODEL script files can be called. The simulator has been set up such that each solid phase has a MODEL script file specific to it. The coding of these MODEL script files is predominantly the same with the difference being in the characterization of the temperature dependent solubility product functions and the form of the $K_{sp}$ equation. Reference to these changes is made in the script files.

Since the MODEL script files all have the same basic structure, the MODEL script for just one of the solid phases (sylvite, KCl) will be reported here along with the PROCESS script that was used for the second case study.

```
# PROCESS script file – NEDMAG

UNIT

  SYL AS SYLVITE          # MODEL file name is SYLVITE
  #HAL AS HALITE
  #BIS AS BISCHOFITE

SET

SYL.T := 298.15 ;   # Setting the temperature to solve at; T has been defined as a variable in MODEL script file

SOLUTIONPARAMETERS
# Defining the solutions parameters – solver to use etc.

  BlockDecomposition := ON ;
  EffectiveZero   := 1.01E-15 ;

  gPLOT  := ON ;
  gRMS   := ON ;
  InitAccuracy := 1E-7;

  LASolver := "MA28"  ;
  MaxInitIterations := 5000 ;
  MaxIterNoImprove  := 1E2 ;
  Monitor := ON  ;
  NStepReductions := 10000 ;
  OutputLevel := 2 ;
```

```
  RelativeAccuracy := 1e-5 ;
#MODEL script file – SYLVITE

PARAMETER
# Defining all known parameters – specifying actual values will follow further on

  Na    AS REAL
  pi    AS REAL
  dw    AS REAL
  e     AS REAL
  Epso  AS REAL
  k     AS REAL
  omega AS REAL
  U1    AS REAL
  U2    AS REAL
  U3    AS REAL
  U4    AS REAL
  U5    AS REAL
  U6    AS REAL
  U7    AS REAL
  U8    AS REAL
  U9    AS REAL
  T     AS REAL
  P     AS REAL
  Betao    AS ARRAY(8) OF REAL # KCl-NaCl-MgCl2-CaCl2-MgSO4-K2SO4-Na2SO4-CaSO4 order
  BetaOne  AS ARRAY(8) OF REAL
  BetaTwo  AS ARRAY(8) OF REAL
  Csi      AS ARRAY(8) OF REAL
  thetao   AS ARRAY(7) OF REAL    # last value in the array is Cl-SO4 interaction
  psio     AS ARRAY(16) OF REAL
  mMgCl    AS ARRAY(20) OF REAL    #interchangeable assignment of which salts molality to set as unknown
  mNaCl    AS ARRAY(20) OF REAL    # defined as an array so can calculate for a number at once
  #mKCl    AS ARRAY(20) OF REAL
  mCaCl    AS ARRAY(20) OF REAL
  mMgSO4   AS ARRAY(20) OF REAL
  mNa2SO4 AS ARRAY(20) OF REAL
  mCaSO4 AS ARRAY(20) OF REAL
  mK2SO4 AS ARRAY(20) OF REAL
  z        AS ARRAY(6) OF REAL      # K-Na-Mg-Ca-Cl-SO4
  consb    AS REAL
  Alpha    AS REAL
  Alpha1   AS REAL
  Alpha2   AS REAL
  Kspsyl AS ARRAY(20) OF REAL   #define as a parameter – temperature dependent function
```

```
VARIABLE
# Define all variables/unknowns– also defined globally, so applicable for all MODEL script files saved in file

  ACK AS ARRAY(20) OF gK
  ACNa AS ARRAY(20) OF gNa
  ACMg AS ARRAY(20) OF gMg
  ACCa AS ARRAY(20) OF gCa
  ACCl AS ARRAY(20) OF gCl
  ACSO4 AS ARRAY(20) OF gSO4
  Etho AS epsilonthousand
  B   AS bee
  C   AS cee
  Eps  AS epsilon
  DebyeHuckelParam   AS Asi
  OsmotCoeff AS ARRAY(20) OF OsmoticCoefficient
  aw     AS ARRAY(20) OF WaterAct
  CNa    AS ARRAY(20) OF mNa
  CK     AS ARRAY(20) OF mK
  CMg    AS ARRAY(20) OF mMg
  CCa    AS ARRAY(20) OF mCa
  CCl    AS ARRAY(20) OF mCl
  CSO4   AS ARRAY(20) OF mSO4
  I      AS ARRAY(20) OF eye
  bigZ   AS ARRAY(20) OF ionicchargealt
  fg     AS ARRAY(20) OF fgamma
  mKCl   AS ARRAY(20) OF ConcK       # in this case solving for the molality of KCl
  x      AS ARRAY(20) OF xee
  xone   AS ARRAY(20) OF xeeone
  xtwo   AS ARRAY(20) OF xeetwo
  g      AS ARRAY(20) OF gee
  gprime  AS ARRAY(20) OF geeprime
  gone    AS ARRAY(20) OF geeone
  gprimeone  AS ARRAY(20) OF geeprimeone
  gtwo    AS ARRAY(20) OF geetwo
  gprimetwo  AS ARRAY(20) OF geeprimetwo

  CKCl   AS potC        #N.B. these are not concentrations
  CNaCl  AS sodC        #but they are the C – constants as defined in the Pitzer model
  CMgCl  AS magC
  CCaCl  AS calC
  CMgSO4  AS magsulC
  CK2SO4  AS potsulC
  CNa2SO4  AS sodsulC
  CCaSO4  AS calsulC
```

```
BsiOne  AS ARRAY(20) OF BsighOne
BsiTwo  AS ARRAY(20) OF BsighTwo
BsiThree AS ARRAY(20) OF BsighThree
BsiFour AS ARRAY(20) OF BsighFour
BsiFive AS ARRAY(20) OF BsighFive
BsiSix AS ARRAY(20) OF BsighSix
BsiSeven AS ARRAY(20) OF BsighSeven
BsiEight AS ARRAY(20) OF BsighEight

BprimeOne  AS ARRAY(20) OF BpriOne
BprimeTwo  AS ARRAY(20) OF BpriTwo
BprimeThree  AS ARRAY(20) OF BpriThree
BprimeFour  AS ARRAY(20) OF BpriFour
BprimeFive  AS ARRAY(20) OF BpriFive
BprimeSix AS ARRAY(20) OF BpriSix
BprimeSeven  AS ARRAY(20) OF BpriSeven
BprimeEight  AS ARRAY(20) OF BpriEight

BnormalOne AS ARRAY(20) OF BnormOne
BnormalTwo AS ARRAY(20) OF BnormTwo
BnormalThree AS ARRAY(20) OF BnormThree
BnormalFour AS ARRAY(20) OF BnormFour
BnormalFive AS ARRAY(20) OF BnormFive
BnormalSix AS ARRAY(20) OF BnormSix
BnormalSeven AS ARRAY(20) OF BnormSeven
BnormalEight AS ARRAY(20) OF BnormEight

F       AS ARRAY(20) OF ff

thetaOnea AS thetonea       #Na-K  interaction
thetaOneb AS thetoneb       #Na-Mg interaction
thetaOnec AS thetonec       #K-Mg interaction
thetaOned AS thetoned       #K-Ca interaction
thetaOnee AS thetonee       #Na-Ca interaction
thetaOnef AS thetonef      #Mg-Ca interaction
thetaOneg AS thetoneg      # Cl-SO4 interaction

PhiOne     AS ARRAY(20) OF fiOne
PhiTwo     AS ARRAY(20) OF fiTwo
PhiThree     AS ARRAY(20) OF fiThree
PhiFour    AS ARRAY(20) OF fiFour
PhiFive    AS ARRAY(20) OF fiFive
PhiSix     AS ARRAY(20) OF fiSix
PhiSeven     AS ARRAY(20) OF fiSeven
```

```
  PhiPrimeOne AS fiPrimeOne
  PhiPrimeTwo AS fiPrimeTwo
  PhiPrimeThree AS fiPrimeThree
  PhiPrimeFour AS fiPrimeFour
  PhiPrimeFive AS fiPrimeFive
  PhiPrimeSix AS fiPrimeSix
  PhiPrimeSeven AS fiPrimeSeven

  PhiSiOne    AS ARRAY(20) OF fiSiOne
  PhiSiTwo    AS ARRAY(20) OF fiSiTwo
  PhiSiThree    AS ARRAY(20) OF fiSiThree
  PhiSiFour    AS ARRAY(20) OF fiSiFour
  PhiSiFive    AS ARRAY(20) OF fiSiFive
  PhiSiSix    AS ARRAY(20) OF fiSiSix
  PhiSiSeven   AS ARRAY(20) OF fiSiSeven

  aK      AS ARRAY(20) OF ActK
  aNa     AS ARRAY(20) OF ActNa
  aMg     AS ARRAY(20) OF ActMg
  aCa     AS ARRAY(20) OF ActCa
  aCl     AS ARRAY(20) OF ActCl
  aSO4    AS ARRAY(20) OF ActSO4

SET
# assign values to all parameters

  Na    := 6.0221367e23 ;
  pi    := 3.1415926 ;
  dw    := 1000 ;
  e     := 1.60217733e-19 ;
  Epso  := 8.854187817e-13 ;
  k     := 1.380658e-23 ;
  omega := 55.51 ;
  P     := 1 ;
  U1    := 3.4279e2 ;
  U2    := -5.0866e-3 ;
  U3    := 9.4690e-7 ;
  U4    := -2.0525 ;
  U5    := 3.1159e3 ;
  U6    := -1.8289e2 ;
  U7    := -8.0325e3 ;
  U8    := 4.2142e6 ;
  U9    := 2.1417 ;
```

# Temperature dependent ion interaction parameters – values taken from Tables 5.1, 5.2

# LOG in g-PROMS is actually the natural logarithm

Betao := [ 2.65718766e1 + 9.92715099e-3 * T - 3.6232333e-6 * T^2 - 6.2842718e-11 * T ^3 - (7.5570722e2 / T) - 4.6730077 * LOG(T), 7.87239712 - 8.3864096e-3 * T + 1.44137774e-5 * T^2 - 8.7820301e-9 * T ^3 - (4.96920671e2 / T) - 8.20972560e-1 * LOG(T), 3.13852913e2 + 2.61769099e-1 * T - 2.4626846e-4 * T^2 + 1.15764787e-7 * T ^3 - (5.53133381e3 / T) - 6.21616862e1 * LOG(T), -5.62764702e1 - 3.00771997e-2 * T + 1.05630400e-5 * T^2 + 3.3331626e-9 * T ^3 + (1.11730349e3 / T) + 1.06664743e1 * LOG(T), 0.1678e1 - 0.5514e-2 * T + 0.597e-6 * T^2 + 0.15651e-7 * T ^3 - (0.22392e3 / T) + 0.6594e-1 * LOG(T), -.7568 + 0.2529e-2 * T + 0.356e-7 * T^2 + 0.531e-9 * T ^3 - (0.108e1 / T) - 0.125e-2 * LOG(T), -0.12709e1 + 0.4425144e-2 * T - 0.35e-8 * T^2 - 0.928e-9 * T ^3 + (0.1425e2 / T) - 0.584e-2 * LOG(T), 0.795e-1 - 0.122e-3 * T + 0.5001e-5 * T^2 + 0.6704e-8 * T ^3 - (0.15228e3 / T) - 0.6885e-2 * LOG(T)] ; # in order KCL - NACL -MGCL- CaCl-MgSO4

BetaOne := [ 1.69742977e3 + 1.22270943 * T - 9.9904449e-4 * T^2 + 4.04786721e-7 * T ^3 - (3.28684422e4 / T) - 3.28813848e2 * LOG(T), 8.66915291e2 + 6.06166931e-1 * T - 4.8048921e-4 * T^2 + 1.88503857e-7 * T ^3 - (1.70460145e4 / T) - 1.67171296e2 * LOG(T), -3.18432525e4 - 2.86710358e1 * T + 2.78892838e-2 * T^2 - 1.3279705e-5 * T ^3 + (5.24032958e5 / T) + 6.40770396e3 * LOG(T), 3.4787 - 1.5417e-2 * T + 3.1791e-5 * T^2 + 0 * T ^3 + (0 / T) + 0 * LOG(T), 0.1484e1 + 0.6274e-2 * T + 0.541e-5 * T^2 + 0.884e-7 * T ^3 - (0.1321e4 / T) + 0.30605 * LOG(T), 0.1953e1 - 0.3996e-2 * T + 0.355e-6 * T^2 + 0.1669e-7 * T ^3 + (0.267e2 / T) - 0.4785e-1 * LOG(T), -0.13915e1 + 0.107532e-1 * T - 0.183e-6 * T^2 - 0.4498e-8 * T ^3 + (0.9328e2 / T) - 0.1678885 * LOG(T), 0.28945e1 + 0.7434e-2 * T + 0.5287e-5 * T^2 - 0.101513e-6 * T ^3 - (0.208505e4 / T) + 0.1345e1 * LOG(T)] ;

BetaTwo := [ 0, 0, 0, 0, 0.18829e3 - 0.103999e1 * T + 0.12242e-2 * T^2 + 0.34974e-5 * T ^3 + (0.8975e5 / T) - 0.679235e2 * LOG(T), 0, 0, -0.5704e2 - 0.1028e-1 * T - 0.2235e-3 * T^2 + 0.3526e-6 * T ^3 + (0.5788e4 / T) - 0.18378e1 * LOG(T)] ;

Csi := [ -3.2757168 - 1.27222054e-3 * T + 4.71374283e-7 * T^2 + 1.1162507e-11 * T ^3 + (9.07747666e1 / T) + 5.80513562e-1 * LOG(T), 1.70761824 + 2.32970177e-3 * T - 2.46665619e-6 * T^2 + 1.2154338e-9 * T ^3 - (1.35583596 / T) - 3.87767714e-1 * LOG(T), 5.9532e-2 - 2.49949e-4 * T + 2.41831e-7 * T^2 + 0 * T ^3 + (0 / T) + 0 * LOG(T), 2.64231655e1 + 2.46922993e-2 * T - 2.4829851e-5 * T^2 + 1.22421864e-8 * T ^3 - (4.18098427e2 / T) - 5.35350322 * LOG(T), 0.2230 - 0.6101e-3 * T - 0.10e-8 * T^2 - 0.1096e-8 * T ^3 + (0.4265e2 / T) - 0.1792e-1 * LOG(T), 0.7e-3 + 0.48e-4 * T + 0.9e-8 * T^2 + 0.326e-9 * T ^3 - (0.768e1 / T) + 0.2835e-2 * LOG(T), 0.21225 - 0.72306e-3 * T + 0 * T^2 - 0.114e-9 * T ^3 + (0.435e1 / T) - 0.1855e-2 * LOG(T), 0.33e-1 - 0.1529e-3 * T + 0.897e-6 * T^2 + 0.1569e-8 * T ^3 + (0.11e1 / T) - 0.12755e-1 * LOG(T)];

thetao := [ -1.82266741e1 - 3.6903847e-3 * T + 0 * T^2 + 0 * T ^3 + (6.12415011e2 / T) + 3.02994981 * LOG(T), 0.07, 0, 2.36571 - 4.540e-3 * T + 0 * T^2 + 0 * T ^3 - (2.84940e2 / T) + 0 * LOG(T), 0.3e-1 - 0.19e-4 * T + 0 * T^2 + 0.95e-9 * T ^3 - (0.25e1 / T) + 0.13e-2 * LOG(T), 5.31274136 - 6.3424248e-3 * T + 0 * T^2 + 0 * T ^3 - (9.83113847e2 / T) + 0 * LOG(T), 0.7e-1 + 0 * T + 0 * T^2 - 0.78e-9 * T ^3 - (0.1e1 / T) + 0 * LOG(T) ] ;

#Interaction parameters in order KNA, NAMG, KMG, KCa, NaCa, MgCa, ClSO4

psio := [ -6.81e-3 + 1.68e-5 * T, 1.99e-2 - (9.51 / T), 2.586E-2 - (14.27 / T), -5.930e-2 + 2.54280e-4 * T + 0 * T^2 + 0 * T ^3 - (1.34390e1 / T) + 0 * LOG(T), -7.6398 - 1.2990e-2 * T + 1.106e-5 * T^2 + 0 * T ^3 + (0 / T) +

```
1.8475 * LOG(T), 4.15790220e1 + 1.30377312e-2 * T + 0 * T^2 + 0 * T ^3 - (9.81658526e2 / T) - 7.4061986 *
LOG(T), -.563e-1 + 0.14146e-2 * T + 0.23e-7 * T^2 - 0.21088e-7 * T ^3 - (0.25661e3 / T) + 0.18538 * LOG(T), -
0.1207 + 0.5235e-3 * T - 0.539e-6 * T^2 - 0.439e-9 * T ^3 - (0.1723e2 / T) + 0.12645e-1 * LOG(T), -0.118 -
0.478e-4 * T - 0.327e-6 * T^2 - 0.937e-9 * T ^3 + (0.3344e2 / T) - 0.884e-2 * LOG(T), 0, -0.808e-1 + 0.46565e-2
* T + 0.5546e-5 * T^2 - 0.14107e-6 * T ^3 - (0.10915e4 / T) + 0.96985 * LOG(T), 0.24e-1, 0.608e-1 - 0.1824e-3 *
T - 0.215e-7 * T^2 - 0.328e-9* T ^3 + (0.522e1 / T) - 0.301e-2 * LOG(T), 0.2554e-1 - 0.6138e-4 * T - 0.90e-8 *
T^2 + 0.304e-9* T ^3 - (0.89 / T) - 0.2275e-2 * LOG(T), 0.5869e-1 - 0.897e-4 * T + 0.47e-7 * T^2 + 0.65e-10*
T ^3 - (0.2413e2 / T) + 0.4345e-2 * LOG(T), - 0.263e-1 - 0.946e-4 * T - 0.3125e-6 * T^2 - 0.128e-8 * T ^3 +
(0.2944e2 / T) - 0.649e-2 * LOG(T)] ;

   z       := [ 1, 1, 2, 2, -1, -2 ] ;          # charge on ions
   mNaCl   :=  6 ;                              #setting this value
   #mKCl   := 1e-5 ;                            # solving for this molality
   mCaCl   := 1e-5 ;
   mMgCl   := [ 0.1, 0.2, 0.3, 0.4, 0.5, 0.6, 0.7, 0.8, 0.9, 1, 1.5, 2, 2.5, 3, 3.5, 4, 4.5, 4.75, 5, 5.5 ]  ;
   # for an array of MgCl molalities
   mMgSO4  := 1e-5 ;
   mK2SO4  := 1e-5 ;
   mNa2SO4 := 1e-5 ;
   mCaSO4  := 1e-5 ;
   consb   := 1.2 ;
   Alpha   := 2 ;
   Alpha1  := 1.4 ;
   Alpha2  := 12 ;
   Kspsyl  := EXP(-1.63e3 - 1.52 * T + 1.45e-3*T^2 – 6.94e-7* T^3 + 2.26e4 / T  + 3.33e2*LOG(T)) ;
   #as defined by parameters in Table 5.3

EQUATION
# Pitzer equations and other required equations

#constants
   Etho = U1 * EXP( U2 * T + U3 * (T^2)) ;
   C    = U4 + ( U5 / (U6 + T) ) ;
   B    = U7 + ( U8 / T ) + U9 * T ;

   Eps  = Etho + C * LOG( ( B + P ) / ( B + 1000 )) ;

   #Debye-Huckel parameter

   DebyeHuckelParam = ( 1 / 3 ) * SQRT( 2 * pi * Na * dw / 1000 ) * ( ( e^2 / ( 4 * pi * Epso * Eps * k * T )) ^ ( 3
/ 2 ) ) ;

#param
   CNa = mNaCl + mNa2SO4;
   CK = mKCl + mK2SO4;
```

```
CMg = mMgCl + mMgSO4 ;
CCa = mCaCl + mCaSO4;

CKCl = Csi(1) / ( 2 * (ABS(z(1) * z(5) ) ^ 0.5 )) ;

CNaCl = Csi(2) / ( 2 * (ABS(z(2) * z(5) ) ^ 0.5 )) ; # constants not concentrations!!!!!

CMgCl = Csi(3) / ( 2 * (ABS(z(3) * z(5) ) ^ 0.5 )) ;

CCaCl = Csi(4) / ( 2 * (ABS(z(4) * z(5) ) ^ 0.5 )) ;

CMgSO4 = Csi(5) / ( 2 * (ABS(z(3) * z(6) ) ^ 0.5 )) ;

CK2SO4 = Csi(6) / ( 2 * (ABS(z(1) * z(6) ) ^ 0.5 )) ;

CNa2SO4 = Csi(7) / ( 2 * (ABS(z(2) * z(6) ) ^ 0.5 )) ;

CCaSO4 = Csi(8) / ( 2 * (ABS(z(4) * z(6) ) ^ 0.5 )) ;

thetaOnea = - thetao(1) / ( 1 + ( Alpha / ( 9 * DebyeHuckelParam))) ;

thetaOneb = - thetao(2) / ( 1 + ( Alpha / ( 9 * 4 * DebyeHuckelParam))) ;

thetaOnec = - thetao(3) / ( 1 + ( Alpha / ( 9 * 4 * DebyeHuckelParam))) ;

thetaOned = - thetao(4) / ( 1 + ( Alpha / ( 9 * 4 * DebyeHuckelParam))) ;

thetaOnee = - thetao(5) / ( 1 + ( Alpha / ( 9 * 4 * DebyeHuckelParam))) ;

thetaOnef = - thetao(6) / ( 1 + ( Alpha / ( 9 * 4 * DebyeHuckelParam))) ;

thetaOneg = - thetao(7) / ( 1 + ( Alpha / ( 9 * 4 * DebyeHuckelParam))) ;

PhiPrimeOne = - 2 * Alpha * thetaOnea / 3 ;

PhiPrimeTwo = - 2 * Alpha * thetaOneb / 3 ;

PhiPrimeThree = - 2 * Alpha * thetaOnec / 3 ;

PhiPrimeFour = - 2 * Alpha * thetaOned / 3 ;

PhiPrimeFive = - 2 * Alpha * thetaOnee / 3 ;

PhiPrimeSix = - 2 * Alpha * thetaOnef / 3 ;
```

```
PhiPrimeSeven = - 2 * Alpha * thetaOneg / 3 ;

FOR h := 1 TO 20 DO

    CCl(h) = mNaCl(h) + mKCl(h) + 2 * mMgCl(h) + 2 * mCaCl(h) ;
        CSO4(h) =  mMgSO4(h) + mK2SO4(h) + mNa2SO4(h) + mCaSO4(h);

#ionic charge

    I(h) = (CK(h) * (z(1)^2) + CNa(h) * (z(2)^2) + CMg(h) * (z(3)^2) + CCa(h) * (z(4)^2) + CCl(h) * (z(5)^2) +
CSO4(h) * (z(6)^2)) / 2 ;

#other paramaters

    bigZ(h) = CNa(h) * ABS(z(2)) + CK(h) * ABS(z(1)) + CMg(h) * ABS(z(3)) + CCa(h) * ABS(z(4)) + CCl(h)
* ABS(z(5)) + CSO4(h) * ABS(z(6)) ;

    fg(h) = - DebyeHuckelParam * (( I(h)^0.5 / (1 + consb * I(h)^0.5)) + (2/consb)* LOG(1 + consb * I(h)^0.5)) ;

      x(h) = Alpha * ( I(h)^0.5 ) ;

      g(h) = 2 * ( 1 - ( 1 + x(h) ) * EXP(-x(h))) / x(h) ^2 ;

      gprime(h) = -2 * ( 1 - ( 1 + x(h) + ( x(h)^2 / 2 )) * EXP(-x(h))) / x(h)^2 ;

      xone(h) = Alpha1 * ( I(h)^0.5 ) ;

      gone(h) = 2 * ( 1 - ( 1 + xone(h) ) * EXP(-xone(h))) / xone(h) ^2 ;

      gprimeone(h) = -2 * ( 1 - ( 1 + xone(h) + ( xone(h)^2 / 2 )) * EXP(-xone(h))) / xone(h)^2 ;

      xtwo(h) = Alpha2 * ( I(h)^0.5 ) ;

      gtwo(h) = 2 * ( 1 - ( 1 + xtwo(h) ) * EXP(-xtwo(h))) / xtwo(h) ^2 ;

      gprimetwo(h) = -2 * ( 1 - ( 1 + xtwo(h) + ( xtwo(h)^2 / 2 )) * EXP(-xtwo(h))) / xtwo(h)^2 ;

      BsiOne(h) = Betao(1) + BetaOne(1) * EXP(-x(h)) ;

      BsiTwo(h) = Betao(2) + BetaOne(2) * EXP(-x(h)) ;

      BsiThree(h) = Betao(3) + BetaOne(3) * EXP(-x(h)) ;


      BsiFour(h) = Betao(4) + BetaOne(4) * EXP(-x(h)) ;
```

```
BsiFive(h) = Betao(5) + BetaOne(5) * EXP(-xone(h)) + BetaTwo(5) * EXP(-xtwo(h)) ;

BsiSix(h) = Betao(6) + BetaOne(6) * EXP(-x(h)) ;

BsiSeven(h) = Betao(7) + BetaOne(7) * EXP(-x(h)) ;

BsiEight(h) = Betao(8) + BetaOne(8) * EXP(-xone(h)) + BetaTwo(8) * EXP(-xtwo(h)) ;

BprimeOne(h) = BetaOne(1) * gprime(h) / I(h) ;

BprimeTwo(h) = BetaOne(2) * gprime(h) / I(h) ;

BprimeThree(h) = BetaOne(3) * gprime(h) / I(h) ;

BprimeFour(h) = BetaOne(4) * gprime(h) / I(h) ;

BprimeFive(h) = (BetaOne(5) * gprimeone(h) + BetaTwo(5) * gprimetwo(h))  / I(h) ;

BprimeSix(h) = BetaOne(6) * gprime(h) / I(h) ;

BprimeSeven(h) = BetaOne(7) * gprime(h) / I(h) ;

BprimeEight(h) = (BetaOne(8) * gprimeone(h) + BetaTwo(8) * gprimetwo(h)) / I(h) ;

BnormalOne(h) = Betao(1) + BetaOne(1) * g(h) ;

BnormalTwo(h) = Betao(2) + BetaOne(2) * g(h) ;

BnormalThree(h) = Betao(3) + BetaOne(3) * g(h) ;

BnormalFour(h) = Betao(4) + BetaOne(4) * g(h) ;

BnormalFive(h) = Betao(5) + BetaOne(5) * gone(h) + BetaTwo(5) * gtwo(h) ;

BnormalSix(h) = Betao(6) + BetaOne(6) * g(h) ;

BnormalSeven(h) = Betao(7) + BetaOne(7) * g(h) ;


BnormalEight(h) = Betao(8) + BetaOne(8) * gone(h) + BetaTwo(8) * gtwo(h) ;

# higher order interactions

PhiOne(h) = thetao(1) + ( 2 * thetaOnea / ( Alpha^2 * I(h))) * ( 1 - ( 1 + x(h) ) * EXP( - x(h) )) ;
```

PhiTwo(h) = thetao(2) + ( 2 * thetaOneb / ( Alpha^2 * I(h))) * ( 1 - ( 1 + x(h) ) * EXP( - x(h) )) ;

PhiThree(h) = thetao(3) + ( 2 * thetaOnec / ( Alpha^2 * I(h))) * ( 1 - ( 1 + x(h) ) * EXP( - x(h) ))

PhiFour(h) = thetao(4) + ( 2 * thetaOned / ( Alpha^2 * I(h))) * ( 1 - ( 1 + x(h) ) * EXP( - x(h) )) ;

PhiFive(h) = thetao(5) + ( 2 * thetaOnee / ( Alpha^2 * I(h))) * ( 1 - ( 1 + x(h) ) * EXP( - x(h) )) ;

PhiSix(h) = thetao(6) + ( 2 * thetaOnef / ( Alpha^2 * I(h))) * ( 1 - ( 1 + x(h) ) * EXP( - x(h) )) ;

PhiSeven(h) = thetao(7) + ( 2 * thetaOneg / ( Alpha^2 * I(h))) * ( 1 - ( 1 + x(h) ) * EXP( - x(h) )) ;

PhiSiOne(h) = PhiOne(h)+ I(h) * PhiPrimeOne ;

PhiSiTwo(h) = PhiTwo(h) + I(h) * PhiPrimeTwo ;

PhiSiThree(h) = PhiThree(h) + I(h) * PhiPrimeThree ;

PhiSiFour(h) = PhiFour(h) + I(h) * PhiPrimeFour ;

PhiSiFive(h) = PhiFive(h) + I(h) * PhiPrimeFive ;

PhiSiSix(h) = PhiSix(h) + I(h) * PhiPrimeSix ;

PhiSiSeven(h) = PhiSeven(h) + I(h) * PhiPrimeSeven ;

F(h) = fg(h) + CK(h) * CCl(h) * BprimeOne(h) + CNa(h) * CCl(h) * BprimeTwo(h) + CMg(h) * CCl(h) * BprimeThree(h) + CCa(h) * CCl(h) * BprimeFour(h) + CMg(h) * CSO4(h) * BprimeFive(h) + CK(h) * CSO4(h) * BprimeSix(h) + CNa(h) * CSO4(h) * BprimeSeven(h) + CCa(h) * CSO4(h) * BprimeEight(h) + CK(h) * CNa(h) * PhiPrimeOne + CMg(h) * CNa(h) * PhiPrimeTwo + CK(h) * CMg(h) * PhiPrimeThree + CK(h) * CCa(h) * PhiPrimeFour + CNa(h) * CCa(h) * PhiPrimeFive + CMg(h) * CCa(h) * PhiPrimeSix + CCl(h) * CSO4(h) * PhiPrimeSeven ;

#osmotic coefficient

OsmotCoeff(h) = 1 + ( 2 / (CK(h) + CNa(h) + CMg(h) + CCl(h) + CCa(h) + CSO4(h))) * ( ( - DebyeHuckelParam * I(h) ^(3/2) / ( 1 + 1.2 * (I(h)^0.5))) + CK(h) * CCl(h) * ( BsiOne(h) + bigZ(h) * CKCl) + CNa(h) * CCl(h) * ( BsiTwo(h) + bigZ(h) * CNaCl) + CMg(h) * CCl(h) * ( BsiThree(h) + bigZ(h) * CMgCl) + CCa(h) * CCl(h) * ( BsiFour(h) + bigZ(h) * CCaCl) + CMg(h) * CSO4(h) * ( BsiFive(h) + bigZ(h) * CMgSO4) + CK(h) * CSO4(h) * ( BsiSix(h) + bigZ(h) * CK2SO4) + CNa(h) * CSO4(h) * (BsiSeven(h) + bigZ(h) * CNA2SO4) + CCa(h) * CSO4(h) * (BsiEight(h) + bigZ(h) * CCaSO4) + CK(h) * CNa(h) * ( PhiSiOne(h) + CCl(h) * psio(1) + CSO4(h) * psio(7)) + CNa(h) * CMg(h) * ( PhiSiTwo(h) + CCl(h) * psio(2) + CSO4(h) * psio(8)) + CK(h) * CMg(h) * ( PhiSiThree(h) + CCl(h) * psio(3) + CSO4(h) * psio(9)) + CK(h) * CCa(h) * ( PhiSiFour(h) + CCl(h) * psio(4) + CSO4(h) * psio(10)) + CNa(h) * CCa(h) * ( PhiSiFive(h) + CCl(h) * psio(5) +

CSO4(h) * psio(11) ) + CCa(h) * CMg(h) * ( PhiSiSix(h) + CCl(h) * psio(6) + CSO4(h) * psio(12)) + CCl(h) * CSO4(h) * ( PhiSiSeven(h) + CMg(h) * psio(15) + CK(h) * psio(13) + CNa(h) * psio(14) + CCa(h) * psio(16))) ;

#activity of water

LOG(aw(h)) = (-OsmotCoeff(h) * (CK(h) + CNa(h) + CMg(h) + CCa(h) + CCl(h) + CSO4(h)) / omega ) ;

#activity coefficients

LOG(ACK(h)) = z(1)^2 * F(h) + CCl(h) * ( 2 * BnormalOne(h) + bigZ(h) * CKCl ) + CSO4(h) * ( 2 * BnormalSix(h) + bigZ(h) * CK2SO4 ) + ABS(z(1))*(CK(h) * CCl(h) * CKCl + CNa(h) * CCl(h) * CNaCl + CMg(h) * CCl(h) * CMgCl + CCa(h) * CCl(h) * CCaCl + CMg(h) * CSO4(h) * CMgSO4 + CK(h) * CSO4(h) * CK2SO4 + CNa(h) * CSO4(h) * CNa2SO4 + CCa(h) * CSO4(h) * CCaSO4) + CNa(h) * ( 2* PhiOne(h) + CCl(h) * psio(1) + CSO4(h) * psio(7)) + CMg(h) * ( 2* PhiThree(h) + CCl(h) * psio(3) + CSO4(h) * psio(9) ) + CCa(h) * ( 2* PhiFour(h) + CCl(h) * psio(4) + CSO4(h) * psio(10)) + CCl(h) * CSO4(h) * psio(13) ;

LOG(ACNa(h)) = z(2)^2 * F(h) + CCl(h) * ( 2 * BnormalTwo(h) + bigZ(h) * CNaCl ) + CSO4(h) * ( 2 * BnormalSeven(h) + bigZ(h) * CNa2SO4 ) + ABS(z(2))*(CNa(h) * CCl(h) * CNaCl + CK(h) * CCl(h) * CKCl + CMg(h) * CCl(h) * CMgCl + CCa(h) * CCl(h) * CCaCl + CMg(h) * CSO4(h) * CMgSO4 + CK(h) * CSO4(h) * CK2SO4 + CNa(h) * CSO4(h) * CNa2SO4 + CCa(h) * CSO4(h) * CCaSO4) + CK(h) * ( 2* PhiOne(h) + CCl(h) * psio(1) + CSO4(h) * psio(7)) + CMg(h) * ( 2* PhiTwo(h) + CCl(h) * psio(2) + CSO4(h) * psio(8) ) + CCa(h) * ( 2* PhiFive(h) + CCl(h) * psio(5) + CSO4(h) * psio(11)) + CCl(h) * CSO4(h) * psio(14) ;

LOG(ACMg(h)) = z(3)^2 * F(h) + CCl(h) * ( 2 * BnormalThree(h) + bigZ(h) * CMgCl ) + CSO4(h) * ( 2 * BnormalFive(h) + bigZ(h) * CMgSO4 ) + ABS(z(3))*(CMg(h) * CCl(h) * CMgCl + CK(h) * CCl(h) * CKCl + CNa(h) * CCl(h) * CNaCl + CCa(h) * CCl(h) * CCaCl + CMg(h) * CSO4(h) * CMgSO4 + CK(h) * CSO4(h) * CK2SO4 + CNa(h) * CSO4(h) * CNa2SO4 + CCa(h) * CSO4(h) * CCaSO4 ) + CNa(h) * ( 2* PhiTwo(h) + CCl(h) * psio(2) + CSO4(h) * psio(8)) + CK(h) * ( 2* PhiThree(h) + CCl(h) * psio(3) + CSO4(h) * psio(9)) + CCa(h) * ( 2* PhiSix(h) + CCl(h) * psio(6) + CSO4(h) * psio(7)) + CCl(h) * CSO4(h) * psio(15);

LOG(ACCa(h)) = z(4)^2 * F(h) + CCl(h) * ( 2 * BnormalFour(h) + bigZ(h) * CCaCl ) + CSO4(h) * ( 2 * BnormalEight(h) + bigZ(h) * CCaSO4 ) + ABS(z(4))*(CCa(h) * CCl(h) * CCaCl + CK(h) * CCl(h) * CKCl + CNa(h) * CCl(h) * CNaCl + CMg(h) * CCl(h) * CMgCl + CMg(h) * CSO4(h) * CMgSO4 + CK(h) * CSO4(h) * CK2SO4 + CNa(h) * CSO4(h) * CNa2SO4 + CCa(h) * CSO4(h) * CCaSO4) + CK(h) * ( 2* PhiFour(h) + CCl(h) * psio(4) + CSO4(h) * psio(10)) + CNa(h) * ( 2* PhiFive(h) + CCl(h) * psio(5) + CSO4(h) * psio(11)) + CMg(h) * ( 2* PhiSix(h) + CCl(h) * psio(6) + CSO4(h) * psio(12)) + CCl(h) * CSO4(h) * psio(16);

LOG(ACCl(h)) = z(5)^2 * F(h) + CK(h) * ( 2 * BnormalOne(h) + bigZ(h) * CKCl) + CNa(h) * ( 2 * BnormalTwo(h) + bigZ(h) * CNaCl ) + CMg(h) * ( 2 * BnormalThree(h) + bigZ(h) * CMgCl ) + CCa(h) * ( 2 * BnormalFour(h) + bigZ(h) * CCaCl ) + CSO4(h) * ( 2 * PhiSeven(h) + CK(h) * psio(13) + CNa(h) * psio(14) + CMg(h) * psio(15) + CCa(h) * psio(16)) + ABS(z(5)) * ( CK(h) * CCl(h) * CKCl + CNa(h) * CCl(h) * CNaCl + CMg(h) * CCl(h) * CMgCl + CCa(h) * CCl(h) * CCaCl + CMg(h) * CSO4(h) * CMgSO4 + CK(h) * CSO4(h) * CK2SO4 + CNa(h) * CSO4(h) * CNa2SO4 + CCa(h) * CSO4(h) * CCaSO4) + CK(h) * CNa(h) * psio(1) + CNa(h) * CMg(h) * psio(2) + CK(h) * CMg(h) * psio(3) + CK(h) * CCa(h) * psio(4) + CNa(h) * CCa(h) * psio(5) + CMg(h) * CCa(h) * psio(6) ;

```
    LOG(ACSO4(h)) =  z(6)^2 * F(h) + CK(h) * ( 2 * BnormalSix(h) + bigZ(h) * CK2SO4) + CNa(h) * ( 2 *
BnormalSeven(h) + bigZ(h) * CNa2SO4 ) + CMg(h) * ( 2 * BnormalFive(h) + bigZ(h) * CMgSO4 ) + CCa(h) * (
2 * BnormalEight(h) + bigZ(h) * CCaSO4 ) + CCl(h) * ( 2 * PhiSeven(h) + CK(h) * psio(13) + CNa(h) * psio(14)
+ CMg(h) * psio(15) + CCa(h) * psio(16)) + ABS(z(6)) * ( CK(h) * CCl(h) * CKCl + CNa(h) * CCl(h) * CNaCl +
CMg(h) * CCl(h) * CMgCl + CCa(h) * CCl(h) * CCaCl + CMg(h) * CSO4(h) * CMgSO4 + CK(h) * CSO4(h) *
CK2SO4 + CNa(h) * CSO4(h) * CNa2SO4 + CCa(h) * CSO4(h) * CCaSO4) + CK(h) * CNa(h) * psio(7) +
CNa(h) * CMg(h) * psio(8) + CK(h) * CMg(h) * psio(9) + CK(h) * CCa(h) * psio(10) + CNa(h) * CCa(h) *
psio(11) + CMg(h) * CCa(h) * psio(12) ;

#solubility
# definitions of activity  - relationship with activity coefficients and molalities defined by equation 1.1

    LOG(aK(h)) = LOG(ACK(h)) + LOG(CK(h)) ;


    LOG(aNa(h)) = LOG(ACNa(h)) + LOG(CNa(h)) ;


    LOG(aMg(h)) = LOG(ACMg(h)) + LOG(CMg(h)) ;


    LOG(aCa(h)) = LOG(ACCa(h)) + LOG(CCa(h)) ;


    LOG(aCl(h)) = LOG(ACCl(h)) + LOG(CCl(h)) ;


    LOG(aSO4(h)) = LOG(ACSO4(h)) + LOG(CSO4(h)) ;

# relating solubities, activities and concentrations

# defining this equation follows on from equations 5.23, 5.24, 5.25

    #Kspsyl(h) = aK(h) * aCl(h);

    LOG(Kspsyl(h)) = LOG(aK(h)) + LOG(aCl(h));
    # same equation written in LOG form – solution convergence easier

END #FOR
```

All the other solid phases have the same layout with their relevant $K_{sp}$ functions as given by Table 5.3. The equations that relate the solubilities, activities and concentrations are also written in the appropriate form in the respective MODEL script files.

# Appendix C – Data Tables

The tables presented here give the data for the 3-dimensional surfaces for the second case study.

*Key*

KCl
NaCl
$MgCl_2.6H2O$
$KCl.MgCl_2.6H2O$

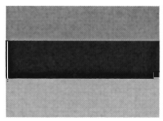

Table A-2: Data for 323K (50°C)

| 323K (50°C) mKCl/mNaCl | 0.58 | 2.84 | 5.52 | 8.06 | 10.47 |
|---|---|---|---|---|---|
| 0.74 | 33.95 | 26.25 | 21.46 | 17.97 | 15.11 |
| 1.47 | 32.46 | 26.19 | 21.38 | 17.89 | 15.02 |
| 2.90 | 30.95 | 26.06 | 21.22 | 17.72 | 14.85 |
| 4.28 | 30.01 | 25.92 | 21.07 | 17.56 | 14.68 |
| 5.63 | 29.30 | 25.79 | 20.91 | 17.39 | 14.51 |
| 6.94 | 27.85 | 25.66 | 20.76 | 17.23 | 14.35 |
| 8.21 | 26.41 | 24.37 | 20.60 | 17.06 | 14.18 |
| 9.45 | 25.14 | 23.15 | 20.45 | 16.90 | 14.02 |
| 10.66 | 23.97 | 22.04 | 19.92 | 16.74 | 13.85 |
| 11.83 | 22.89 | 21.01 | 18.94 | 16.58 | 13.69 |
| 12.98 | 21.88 | 20.05 | 18.03 | 16.25 | 13.53 |

Table A-3: Data for 313K (40°C)

| 313K (40°C) mKCl/mNaCl | 0.58 | 2.84 | 5.52 | 8.06 | 10.47 |
|---|---|---|---|---|---|
| 0.74 | 32.73 | 25.87 | 21.14 | 17.70 | 14.86 |
| 1.47 | 31.32 | 25.80 | 21.06 | 17.61 | 14.77 |
| 2.90 | 29.86 | 25.66 | 20.90 | 17.43 | 14.59 |
| 4.28 | 28.95 | 25.52 | 20.73 | 17.26 | 14.41 |
| 5.63 | 27.29 | 25.22 | 20.57 | 17.08 | 14.23 |
| 6.94 | 25.59 | 23.60 | 20.40 | 16.91 | 14.05 |
| 8.21 | 24.14 | 22.21 | 20.07 | 16.73 | 13.87 |
| 9.45 | 22.84 | 20.96 | 18.88 | 16.56 | 13.69 |
| 10.66 | 21.65 | 19.82 | 17.80 | 16.00 | 13.52 |
| 11.83 | 20.54 | 18.76 | 16.79 | 15.03 | 13.34 |
| 12.98 | 19.49 | 17.76 | 15.83 | 14.13 | 12.60 |

Table A-4: Data for 303K (30°C)

| 303K (30°C) mKCl/mNaCl | 0.58 | 2.84 | 5.52 | 8.06 | 10.47 |
|---|---|---|---|---|---|
| 0.74 | 31.63 | 25.54 | 20.87 | 17.46 | 14.66 |
| 1.47 | 30.28 | 25.46 | 20.78 | 17.37 | 14.56 |
| 2.90 | 28.86 | 25.32 | 20.61 | 17.18 | 14.36 |
| 4.28 | 27.17 | 25.12 | 20.44 | 17.00 | 14.17 |
| 5.63 | 25.08 | 23.12 | 20.26 | 16.81 | 13.97 |
| 6.94 | 23.36 | 21.47 | 19.36 | 16.62 | 13.78 |
| 8.21 | 21.88 | 20.04 | 17.99 | 16.15 | 13.58 |
| 9.45 | 20.55 | 18.76 | 16.76 | 14.97 | 13.35 |
| 10.66 | 19.33 | 17.58 | 15.63 | 13.89 | 12.31 |
| 11.83 | 18.19 | 16.49 | 14.58 | 12.88 | 11.34 |
| 12.98 | 17.11 | 15.44 | 13.58 | 11.92 | 10.42 |

Table A-5: Data for 298K (25°C)

| 298K (25°C) mKCl/mNaCl | 0.58 | 2.84 | 5.52 | 8.06 | 10.47 |
|---|---|---|---|---|---|
| 0.74 | 31.12 | 25.40 | 20.76 | 17.37 | 14.57 |
| 1.47 | 29.79 | 25.32 | 20.67 | 17.27 | 14.47 |
| 2.90 | 28.40 | 25.17 | 20.49 | 17.08 | 14.27 |
| 4.28 | 26.09 | 24.10 | 20.31 | 16.88 | 14.06 |
| 5.63 | 23.99 | 22.07 | 19.93 | 16.69 | 13.86 |
| 6.94 | 22.26 | 20.40 | 18.33 | 16.47 | 13.66 |
| 8.21 | 20.76 | 18.96 | 16.94 | 15.12 | 13.45 |
| 9.45 | 19.41 | 17.66 | 15.69 | 13.92 | 12.32 |
| 10.66 | 18.17 | 16.46 | 14.54 | 12.81 | 11.25 |
| 11.83 | 17.01 | 15.34 | 13.46 | 11.77 | 10.25 |
| 12.98 | 15.92 | 14.28 | 12.44 | 10.79 | 9.30 |

Table A-6: Data for 283K (25°C)

| 283K (10°C) mKCl/mNaCl | 0.58 | 0.03 | 0.06 | 0.08 | 0.10 |
|---|---|---|---|---|---|
| 0.74 | 29.79 | 25.10 | 20.53 | 17.19 | 14.43 |
| 1.47 | 28.52 | 25.02 | 20.44 | 17.08 | 14.31 |
| 2.90 | 25.80 | 23.81 | 20.24 | 16.87 | 14.08 |
| 4.28 | 22.95 | 21.06 | 18.94 | 16.65 | 13.85 |
| 5.63 | 20.78 | 18.97 | 16.91 | 15.06 | 13.37 |
| 6.94 | 19.00 | 17.23 | 15.23 | 13.42 | 11.77 |
| 8.21 | 17.44 | 15.72 | 13.76 | 11.99 | 10.38 |
| 9.45 | 16.04 | 14.35 | 12.43 | 10.70 | 9.11 |
| 10.66 | 14.74 | 13.09 | 11.20 | 9.50 | 7.94 |
| 11.83 | 13.53 | 11.90 | 10.05 | 8.37 | 6.84 |
| 12.98 | 12.37 | 10.77 | 8.94 | 7.29 | 5.79 |